Lehigh University
Lehigh Preserve

Theses and Dissertations

1973

Dynamic and static fracture toughness of Ti-6A1-4v

G. F. Mitchell
Lehigh University

Follow this and additional works at: https://preserve.lehigh.edu/etd

 Part of the Materials Science and Engineering Commons

Recommended Citation
Mitchell, G. F., "Dynamic and static fracture toughness of Ti-6A1-4v" (1973). *Theses and Dissertations*. 4096.
https://preserve.lehigh.edu/etd/4096

This Thesis is brought to you for free and open access by Lehigh Preserve. It has been accepted for inclusion in Theses and Dissertations by an authorized administrator of Lehigh Preserve. For more information, please contact preserve@lehigh.edu.

DYNAMIC AND STATIC FRACTURE TOUGHNESS OF Ti-6Al-4V

Lcdr. G. F. Mitchell, USN

A Thesis

Presented to the Graduate Committee

of Lehigh University

in Candidacy for the Degree of

Master of Science

in

Metallurgy and Materials Science

Lehigh University

1972

CERTIFICATE OF APPROVAL

This thesis is accepted and approved in partial fulfillment of the requirements for the degree of Master of Science.

November 13, 1972
(date)

Allan O Pierce
Professor in Charge

C. F. Conrad
Chairman

ACKNOWLEDGEMENTS

Grateful appreciation is extended to:

Dr. Alan W. Pense whose guidance during this investigation was most valuable.

The Office of Naval Research for financial assistance.

The Naval Research Laboratory for supplying the test material.

Gopala Krishna for his insight and assistance in conducting the dynamic tests.

TABLE OF CONTENTS

LIST OF TABLES

LIST OF FIGURES

ABSTRACT

Room temperature dynamic and static fracture toughness tests were conducted on the alloy Ti-6Al-4V in one-inch thick section. Several conditions of heat treatment were investigated including one in which the material was severely overaged. In the dynamic tests, a simply supported beam type specimen was subjected to impact loading, the force of which was electronically recorded as a function of time. Dynamic plane strain fracture toughness (K_{1D}) and dynamic tear (DT) energy was calculated from the force-time record. A calibrated energy absorption system was used as a secondary means for the determination of DT energy. Static fracture toughness was obtained from standard K_{1C} tests which differed from the dynamic tests by about four orders of magnitude in strain rate.

In all cases the dynamic plane strain fracture toughness was approximately double that for the static case, a trend quite opposite to that generally observed in steel. It was found that K_{1D} could be analytically related to DT energy through strain energy release rate. K_{1D} levels of 90-125 ksi-$in^{\frac{1}{2}}$ were predicted from DT energy and tensile data with an accuracy of approximately 10%. High strain rate yield strength of the alloy was approximated with numerical descriptions of temperature and strain rate effects on plain carbon steels, which were experimentally determined to be generally applicable to Ti-6Al-4V. Long-time, high-temperature overageing significantly reduced the fracture toughness of this alloy, having little effect on its static yield strength.

INTRODUCTION

The titanium alloy 6-aluminum, 4-vanadium is considered to be the "work-horse" of the titanium alloys. In 1971, Ti-6Al-4V accounted for 56% of the 30 million pounds of titanium and titanium alloys commercially produced.[1] Its high strength to weight ratio (6.25×10^5 in.) makes it most attractive to the aerospace industry which is in fact the major consumer. Although equally attractive to many other areas of application, its high cost has made the alloy non-competitive with respect to other strong materials such as the high strength steels and copper-nickel alloys. However, the trend in cost reduction from $15/pound in 1956 to $5/pound in 1966 to a current cost of $3-$4/pound is expected to continue, making the alloy competitive on a first cost basis and superior from a life cycle standpoint.[2] For the past decade the marine industry in particular has had an interest in Ti-6Al-4V because of its good fatigue properties and corrosion/erosion resistance. Poor weldability is also a primary obstacle to more extensive use.

Metallurgically, Ti-6Al-4V is a two phase precipitation strengthened alloy. Precipitation strengthened is more descriptive than precipitation hardened since only modest changes in hardness occur with heat treatment. The high temperature (beta) phase is body-centered cubic and is stabilized by vanadium in this alloy. Alpha is the low (room) temperature phase, having a hexagonal close-packed

structure which is stabilized and solution strengthened by aluminum. Both of the principle alloying elements form substitutional solid solutions with titanium.[3] A 5.5% Al isopleth of the Ti-Al-V ternary system is shown in Figure 1.[4] In practice the alloy behaves very much like a "beta isomorphous" system in which normal deviations from equilibrium cooling result in an annealed structure of primary alpha particles in a beta matrix.[5]

The phase changes occurring during solution treatment and ageing are quite complex and detailed discussion is beyond the scope of this thesis. Briefly, solution treatment results in two to four metastable structures depending on the temperature from which the alloy is quenched. From temperatures near the beta transus (1800°F), quenching results in a hexagonal close-packed martensite (α''), supersaturated beta and vanadium depleted alpha. During ageing, alpha and beta precipitate from α'' and diffusion leads to a more stable alpha-beta mixture. Quenching from lower temperatures such as 1550°F results in a face-centered cubic martensite (α') rather than the α'' discussed above. Ageing results in the reversion of α' to beta, from which alpha precipitates. Quenching from 1640°F to 1700°F can result in all four structures, i.e., α'', α', supersaturated beta and depleted alpha. Solution treatment above the beta transus is not generally practiced because it results in a significant loss of ductility.[6,7]

Because of the popularity of the alloy, Ti-6Al-4V has been extensively tested. The Defense Metals Information Center of the Battelle Memorial Institute has served as a clearing house for much of the research and has published a large series of reports on the

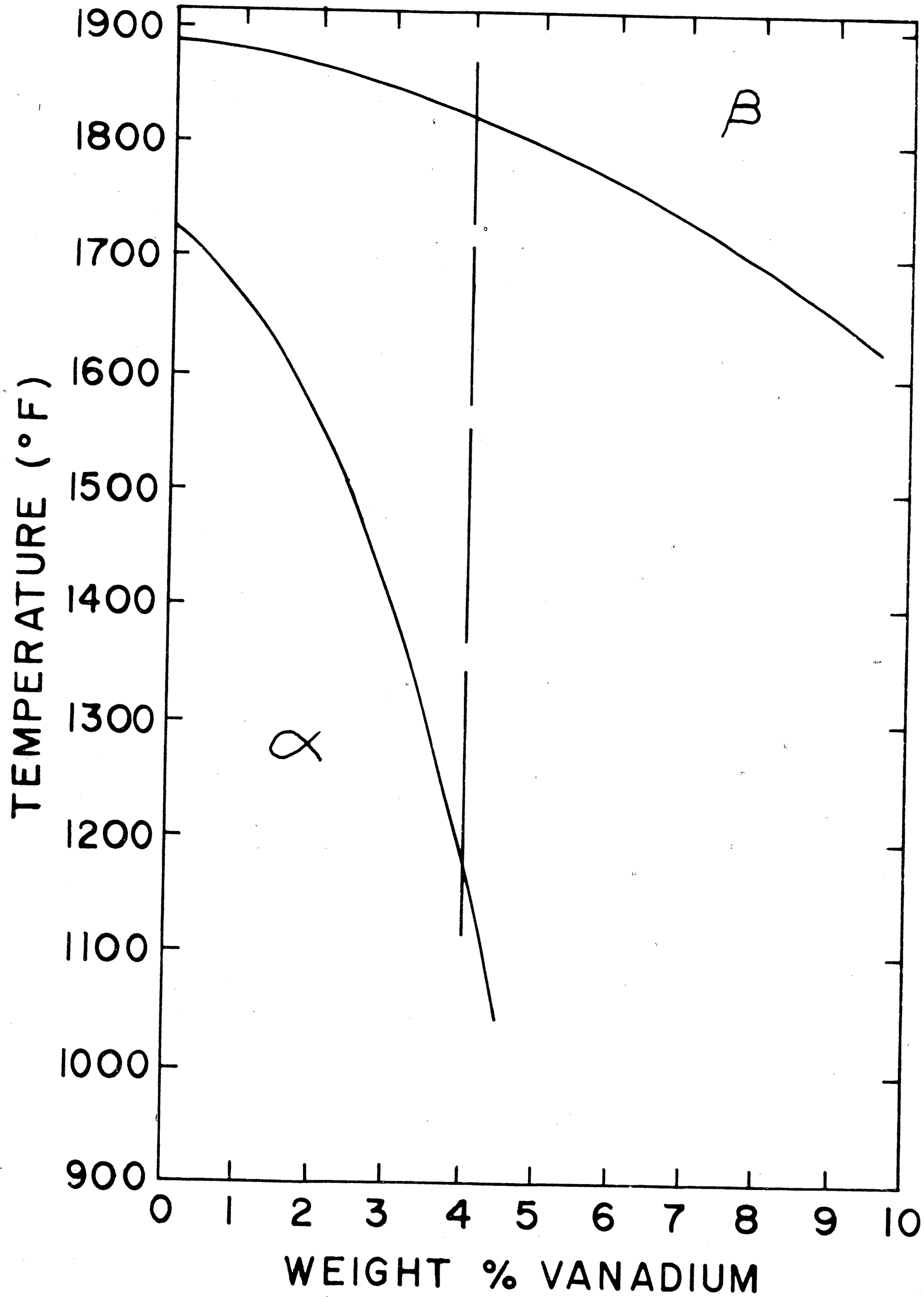

Figure 1 — Vertical Section of the Ti-Al-V Ternary System at 5.5% Al (Ref. 4)

alloy over the past two decades. The Naval Research Laboratory, Washington, D.C. has also done a considerable amount of testing of titanium alloys, including, of course, Ti-6Al-4V.[8] Many other research efforts in addition to these have resulted in an abundance of data for the alloy. Still, a great many questions remain unanswered and research continues in almost every aspect of the alloy's behavior.

It is the fracture toughness of Ti-6Al-4V that is the focus of the research resulting in this thesis. A dilemma exists in this area because there are two widely accepted and equally justifiable fracture toughness testing methods which do not compare well with each other from an analytical standpoint. One is the Dynamic Tear (DT) test which involves the measurement of energy expenditure to achieve fracture by dynamic loading.[9] The other is plane strain fracture toughness, a static test the result of which is a parameter called stress intensity factor (K_{1C}) that indicates the combined effects of the externally applied load and the inherent crack size required for fracture.[10] There are five significant differences between the DT and K_{1C} tests:

1. Strain Rate: the static K_{1C} test strain rate differs from that of the DT test by approximately four orders of magnitude (10^{-1} to 10^{3} in^{-1}).[11]
2. Property Measured: K_{1C} is generally considered to be a fracture initiation parameter while DT energy includes both initiation and propagation.
3. Cost: a K_{1C} test costs approximately \$100 and is relatively complex compared to the simple DT test which costs about \$10.[12]

4. Testable Range: the K_{1C} test yields a valid number only for the higher strength, less ductile materials. The DT test is applicable to the full range of fracture toughness, from fully brittle to fully ductile.
5. Application in Design: design engineers typically work with allowable stresses and do not find fracture energy to be very useful in design analysis. A maximum allowable stress can be obtained from K_{1C} if the largest crack size involved is either known or can be determined.

Figure 2 is a graph of the correlation between DT and K_{1C} for a variety of titanium alloys as determined by the Naval Research Laboratory (NRL).[12] The scatter in data is acceptable considering material and experimental variations as well as the lack of exactness inherent in the DT test. The correlation in Figure 2 indicates that a definite trend exists and that approximate K_{1C} values can be obtained from DT tests.

It is on the basis of strain energy release rate (G) that K_{1C} and DT energy fail to coincide. This parameter is a measure of the strain energy released to form a unit area of fracture surface and is derived from the Griffith theory of crack growth. Strain energy release rate can be related to K_{1C} mathematically by the equation:[13]

$$G_{1C} = \frac{K_{1C}^2}{E}(1-u^2) \qquad (1)$$

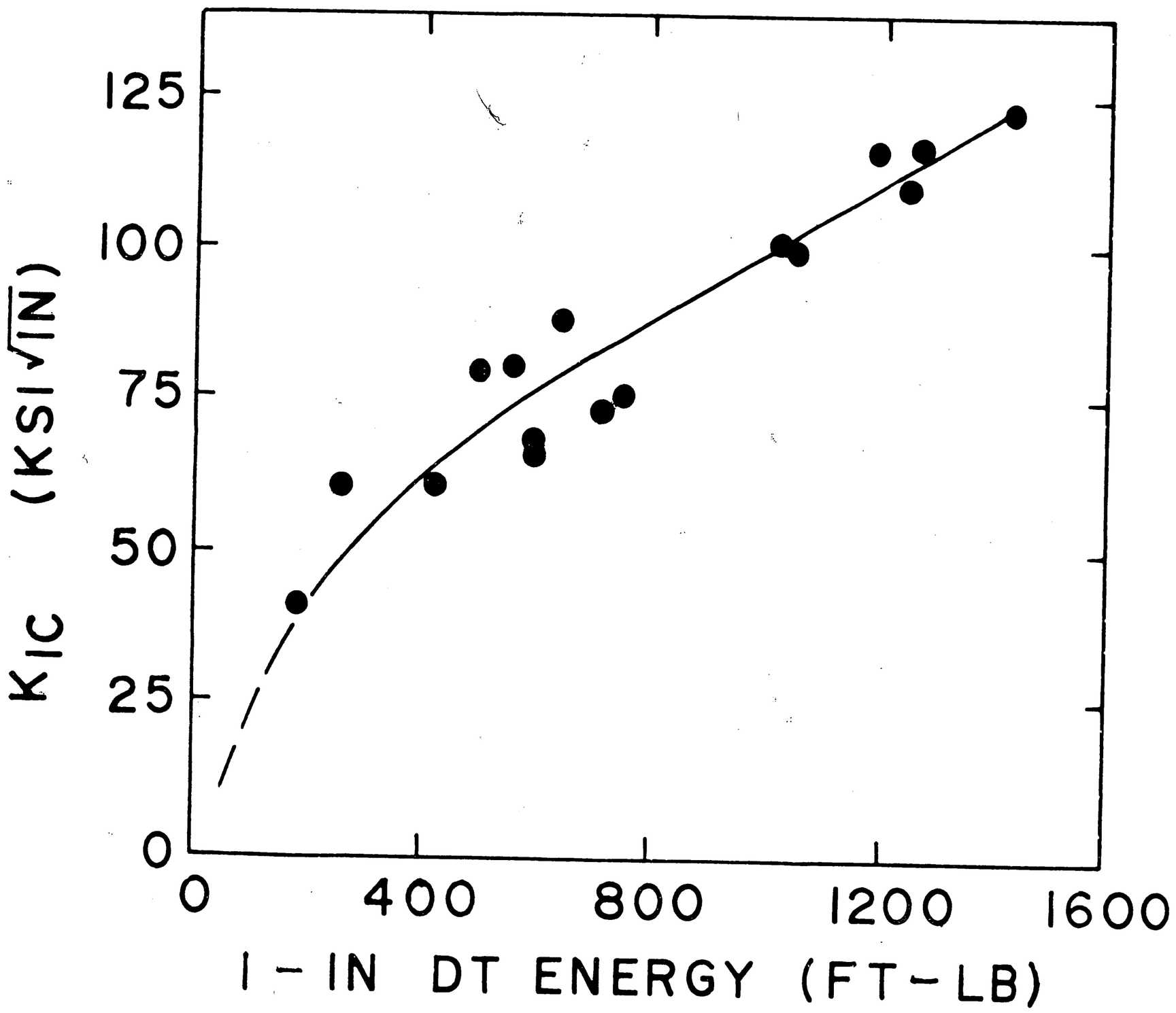

Figure 2 — Experimental Correlation of DT Energy and K_{IC} for 1-in. and 3-in. Thick Titanium Alloys (Ref. 12)

where G_{1C} = strain energy release rate, psi-in.

K_{1C} = plane strain fracture toughness, psi-$in^{\frac{1}{2}}$

E = elastic modulus, psi

u = Poisson's ratio

G may also be related to DT by:

$$G_{DT} = \frac{DT}{2A} \tag{2}$$

where DT = Dynamic Tear Energy, in-lbs

A = area of fracture, in^2

The factor of 2 accounts for the formation of two fracture surfaces.

It seems apparent that G_{1C} would equal G_{DT} only in the case in which strain rate did not affect the energy required for fracture. Even in this unrealistic case the two would probably not coincide over the full range of fracture toughness because, as previously mentioned, K_{1C} is a fracture initiation parameter while DT energy includes both initiation and propagation. That is, it may require more or less energy to initiate fracture than it does for fracture to continue once propagation has begun. It is reasonable to assume that the ratio of G_{1C} to G_{DT} may be as high as two for brittle materials and as low as one half for ductile materials. Then at some point in the range of fracture toughness, were it not for the strain rate effect, the ratio should be one and DT should be related to K_{1C} by:

$$\frac{K_{1C}^2}{E}(1-u^2) = \frac{DT}{2A} \tag{3}$$

Figures 3, 4, and 5 are Naval Research Laboratory graphs of G_{1C} versus DT/2A for a variety of titanium, steel, and aluminum alloys, respectively.[8,14,15] G_{1C} in each case was determined by a modified form of equation (1), specifically:

$$G_{1C} = \frac{K_{1C}^2}{E} \qquad (4)$$

The $(1-u^2)$ term if included would alter the graphs only slightly. Superimposed on each graph is a line representing the conditions of equation (3), with the $(1-u^2)$ term again neglected. It is obvious that in these materials, representing a substantial range of fracture toughness, G_{1C} is considerably less than G_{DT}. The ratio of G_{1C} to G_{DT} is in fact .5, .25, and .2 for titanium, steel and aluminum alloys, respectively.

While it is certainly worthwhile to have experimental correlations such as that between K_{1C} and DT shown in Figure 2, it is preferable that an analytical relationship be established, however approximate. In view of the significant difference in strain rate between the DT and K_{1C} tests it seems unreasonable to expect the two to be analytically relatable without including a strain rate factor such as nominal strain rate ($\dot{e}$) or crack tip stress rate factor ($\dot{K}$). An alternative would be to establish a dynamic plane strain fracture toughness (K_{1D}) test with strain rates on the same order as that of the DT test. It may then be possible to relate K_{1C} to K_{1D} through some strain rate parameter. An additional impetus for the development of a K_{1D} test lies in the speculation that K_{1D} may be a better parameter than K_{1C} on which to base design.[16]

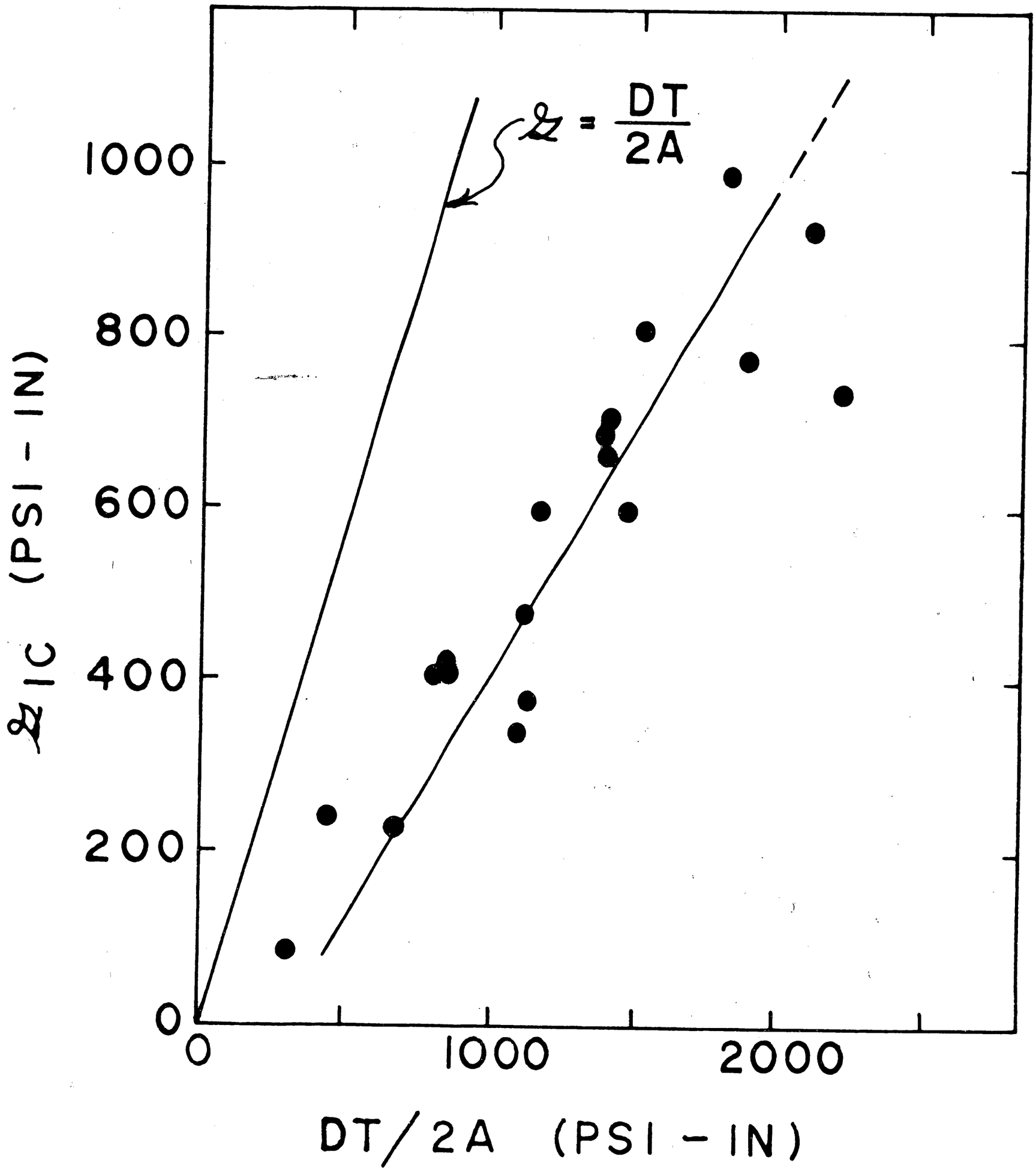

Figure 3 — Correlation of Strain Energy Release Rate and DT Energy Per Unit Fracture Surface for 1-in. Thick Titanium Alloys (Ref. 8)

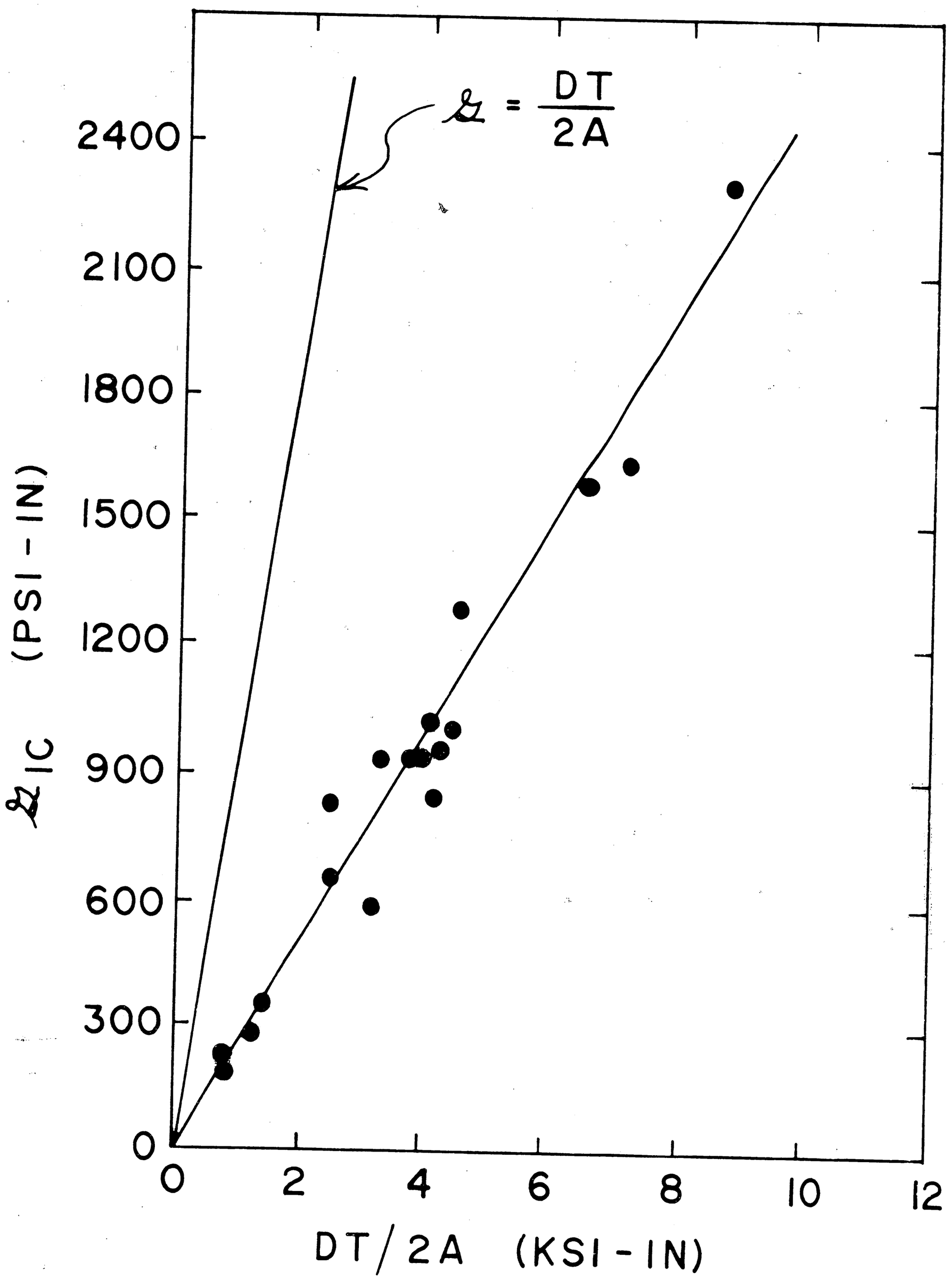

Figure 4 — Correlation of Strain Energy Release Rate and DT Energy Per Unit Fracture Surface for Steel Alloys (Ref. 14)

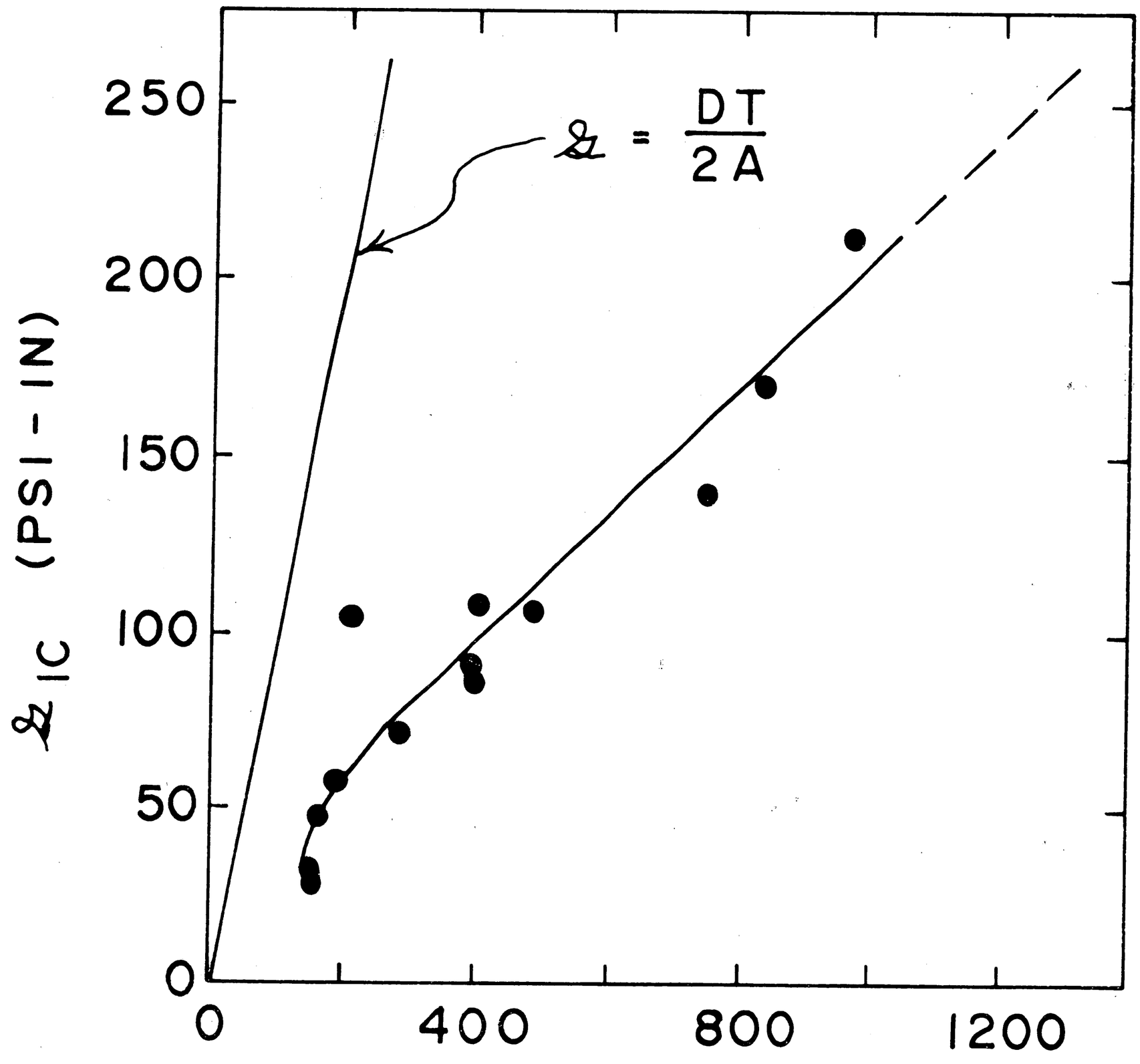

Figure 5 — Correlation of Strain Energy Release Rate and DT Energy Per Unit Fracture Surface for Aluminum Alloys (Ref. 15)

Dynamic plane strain fracture toughness testing has been attempted but it is in the infancy stage and standards have not been established as they have for the DT and K_{1C} tests. Preliminary research on mild steel indicates a decreasing trend of plane strain fracture toughness with increased loading rates. Similar work with Ti-6Al-4V indicates an opposite effect, the fracture toughness being nearly doubled by impact as opposed to static testing.[17] Apparently no effort has been made to pursue the matter for titanium alloys, particularly in relating DT to K_{1D}. However, additional work has been done for steels and numerical descriptions have been developed for temperature and strain rate effects on their plane strain fracture toughness.[18]

Still another alternative would be to slow down the DT test to strain rates equivalent to K_{1C} testing. This condition has been approached by slow bend pre-cracked Charpy tests on titanium alloys.[19] These tests have yielded rather good results in terms of equation (3), but it appears that the excellent correlation may be attributed to the fact that the tests very much approach the standard bend test for K_{1C}.[20] A simple test such as the DT test still appears desirable from an economic standpoint, if its results can be translated into a design stress.

The primary objective on this research was to determine if, on the basis of strain energy release rate, DT values could be related to the dynamic plane strain fracture toughness of the alloy Ti-6Al-4V. If this relationship were found to exist, more extensive use of the simple and economical DT test may be possible. Of nearly equal importance was verification of the fact that for this alloy, the energy requirements

for dynamic fracture are much higher than those for the static case. Also of interest were correlations between K_{1C}, K_{1D}, yield strength, elastic modulus and combinations thereof.

TEST MATERIAL

Characterization

The material tested was a commercial grade Ti-6Al-4V alloy with the chemical analysis shown in Table I. It should be noted that the

ELEMENT	CONTENT (Wt %)
Aluminum	6.5
Vanadium	4.2
Carbon	0.02
Nitrogen	0.012
Iron	0.18
Oxygen	0.18
Hydrogen	<100 PPM

Table I — Chemical Analysis of Test Material

oxygen content is 0.18%. An ELI (extra low interstitial) grade of this alloy with oxygen contents between 0.10% and 0.13% is also commercially available. The ELI grade has been shown to exhibit superior fracture toughness compared to the standard commercial grade which has oxygen contents of 0.15% to 0.20%. Oxygen is contained in the alloy for increased strength but tends to cause embrittlement when it is present in excess of approximately 0.13%.[21]

The test material was produced by Reactive Metals Incorporated (HT #304147) in the form of mill annealed plate with a nominal thickness of one inch. The Naval Research Laboratory provided the

material for this investigation, precut into 18 in. by 4.75 in. blanks, the size required for the 1 in. DT test. The 4.75 in. dimension was the direction of primary rolling although the composite photomicrograph shown in Figure 6 suggests that the material was cross-rolled. Figure 7, a photomicrograph of the as-received material at high magnification reveals a structure of elongated alpha grains in a beta matrix, typical of the annealed alloy.[22]

Preliminary tests were conducted for characterization of the as-received material. The results of these tests are shown in Table II.

	TEST DIRECTION	
	Longitudinal	Transverse
Yield Strength (ksi)	128.8	141.1
Tensile Strength (ksi)	137.2	148.5
Total Elongation (%)	14.1	14.1
Elastic Modulus (msi)	16.7	18.4

Table II — Tensile Properties of As-Received Material

Note that superior tensile properties in the transverse direction, though not the usual case, has been reported by previous investigators of this alloy.[23,24,25]

Heat Treatment

In order to make the desired correlation, it was necessary to obtain a range in the fracture toughness behavior of the alloy. The first impulse was to conduct tests at a variety of low temperatures

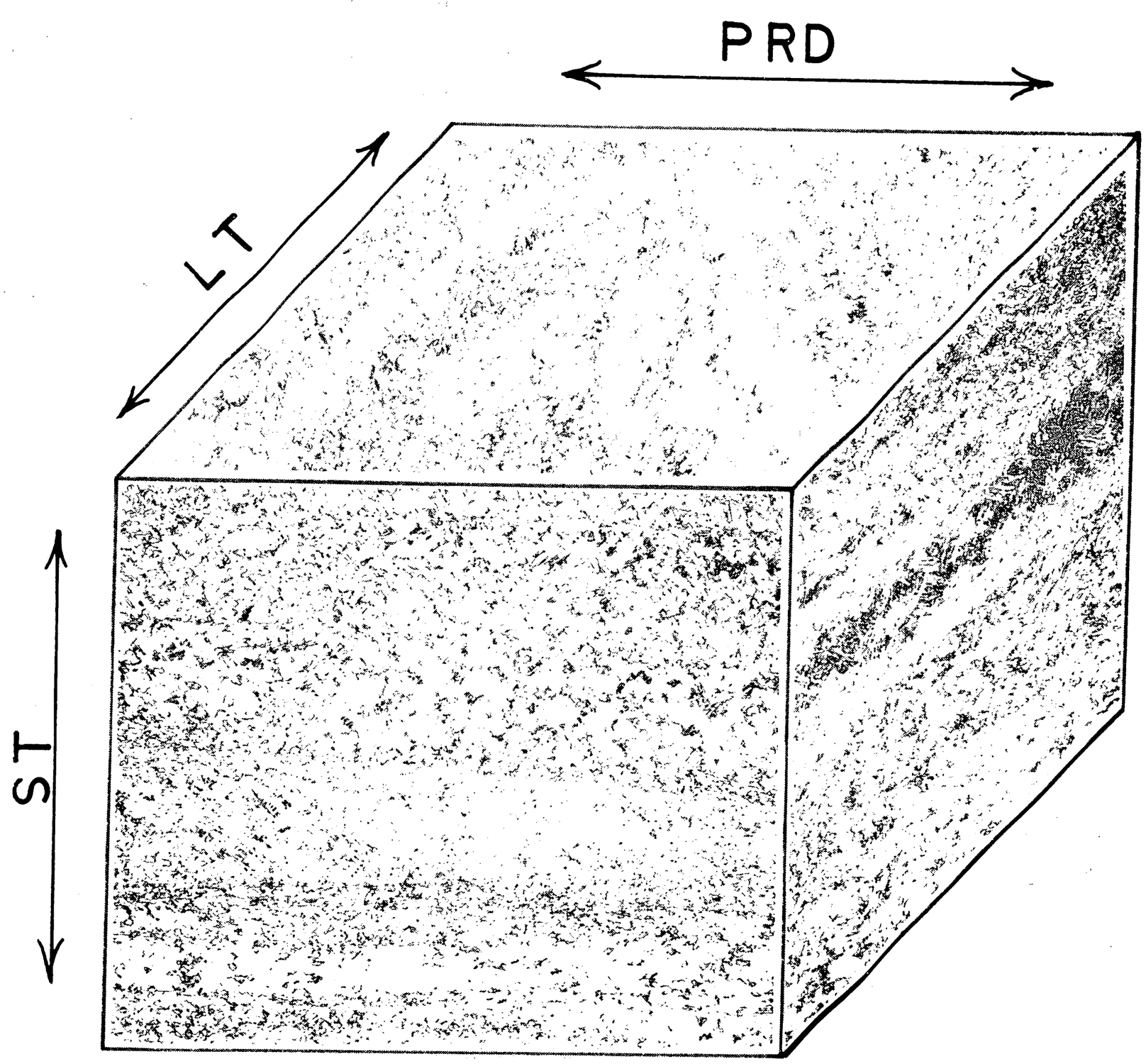

Figure 6 — Composite Photomicrograph of Test Material Indicating Cross-Rolled Microstructure

(Mag: 67X - Etchant: 10% HF/5% HNO_3)

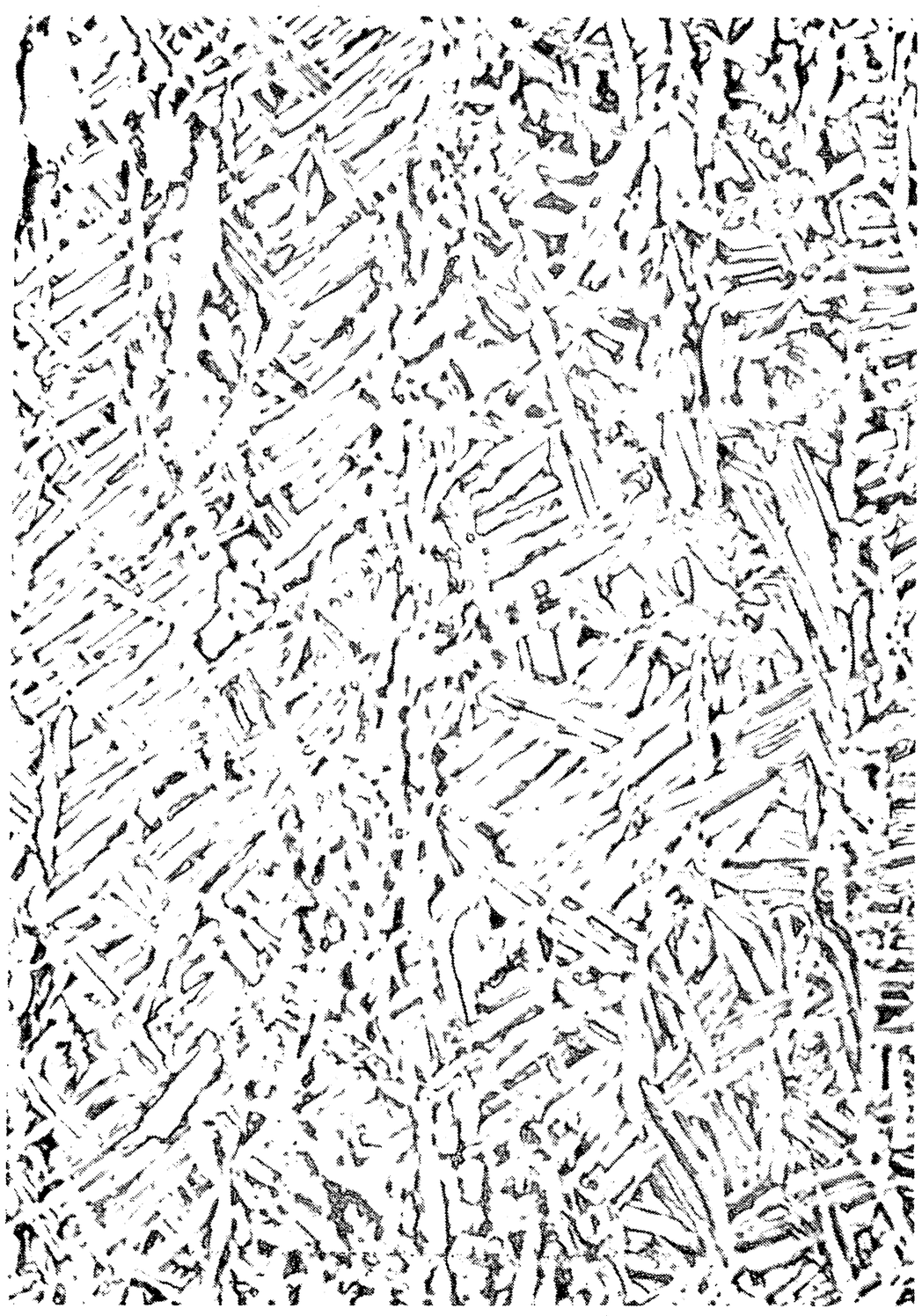

Figure 7 — Photomicrograph Revealing the Structure of the As-Received Material

(Mag: 800X - Etchant: 10% HF/5% HNO_3)

since this is known to significently affect the fracture toughness of most materials. However, previous researchers had found that while the yield strength of this alloy was quite temperature sensitive, its fracture toughness is only moderately affected by low temperatures.[26]

The next logical approach to obtaining the desired range in fracture toughness was through heat treatment. The fracture toughness of titanium alloys generally decreases with increasing yield strength although the correlation is quite inexact.[6,8] It was therefore assumed that some variation in fracture toughness could be obtained by heat treating the alloy to various levels of yield strength. It has also been found that long time, high temperature ageing of this alloy reduced its fracture toughness by approximately 40%.[27] This offered a means for achieving minimal fracture toughness values.

Preliminary heat treatments and tensile tests were conducted to determine the maximum range of yield strength obtainable. The effect of heat treatment variables on the yield strength of Ti-6Al-4V has been well documented so that a minimum of guesswork was required.[28,29,30] The final heat treatments selected and the corresponding yield strengths obtained are shown in Table III. It should be emphasized

Solution Treatment	Ageing Treatment	Yield Strength
1650°F/1hr/WQ	None	126 ksi
1650°F/1hr/WQ	1300°F/8hr/AC	142 ksi
1650°F/1hr/WQ	1000°F/8hr/AC	154 ksi
1750°F/1hr/WQ	925°F/2hr/AC	162 ksi
1650°F/1hr/WQ	1100°F/96hr/AC	153 ksi

Table III — Selected Heat Treatments and Yield Strengths Obtained

that the preliminary heat treatments were conducted on tensile specimen blanks with ½ in. square cross-sections. As will be seen later, the full thickness (1 in.) plates did not have the same response to heat treatment.

Twenty 1 in. thick DT blanks were provided by the Naval Research Laboratory. Eighteen of these were heat treated to the yield strength levels indicated in Table III. The specimen identification numbers for each level is shown in Table IV. Solution treatments were given in a

Yield Strength Level (ksi)	Specimen #
126	1,2,3,4
142	5,6,7,8
154	9,10,11,12
162	13,14,15
153 (overaged)	16,17,18

Table IV — Identification of 1 in. DT-K_{1D} Specimens and Yield Strength Levels to which Heat Treated

Lucifer Model 3027 F furnace which had a capacity for a maximum of five specimen blanks. An argon atmosphere was provided at a flow rate of 30 ft^3/min. After solution treatment the blanks were given an agitated quench in a 70 gallon tank of water at room temperature, the delay time from furnace to tank being less than two seconds. Heat-up of the water by successive quenching resulted in the fifth specimen being quenched in tepid water. Ageing treatments were given in a Hevi-Duty Type HD-122412-CUA furnace with no protective atmosphere provided. Only mild discolorization and flaking were noted after heat treatment.

Specimen Orientation

Except for characterization tests of the as-received material, all testing was done with specimens oriented such that the plane of fracture was normal to the long transverse direction. This is commonly referred to as the WR orientation and is illustrated in Figure 8.

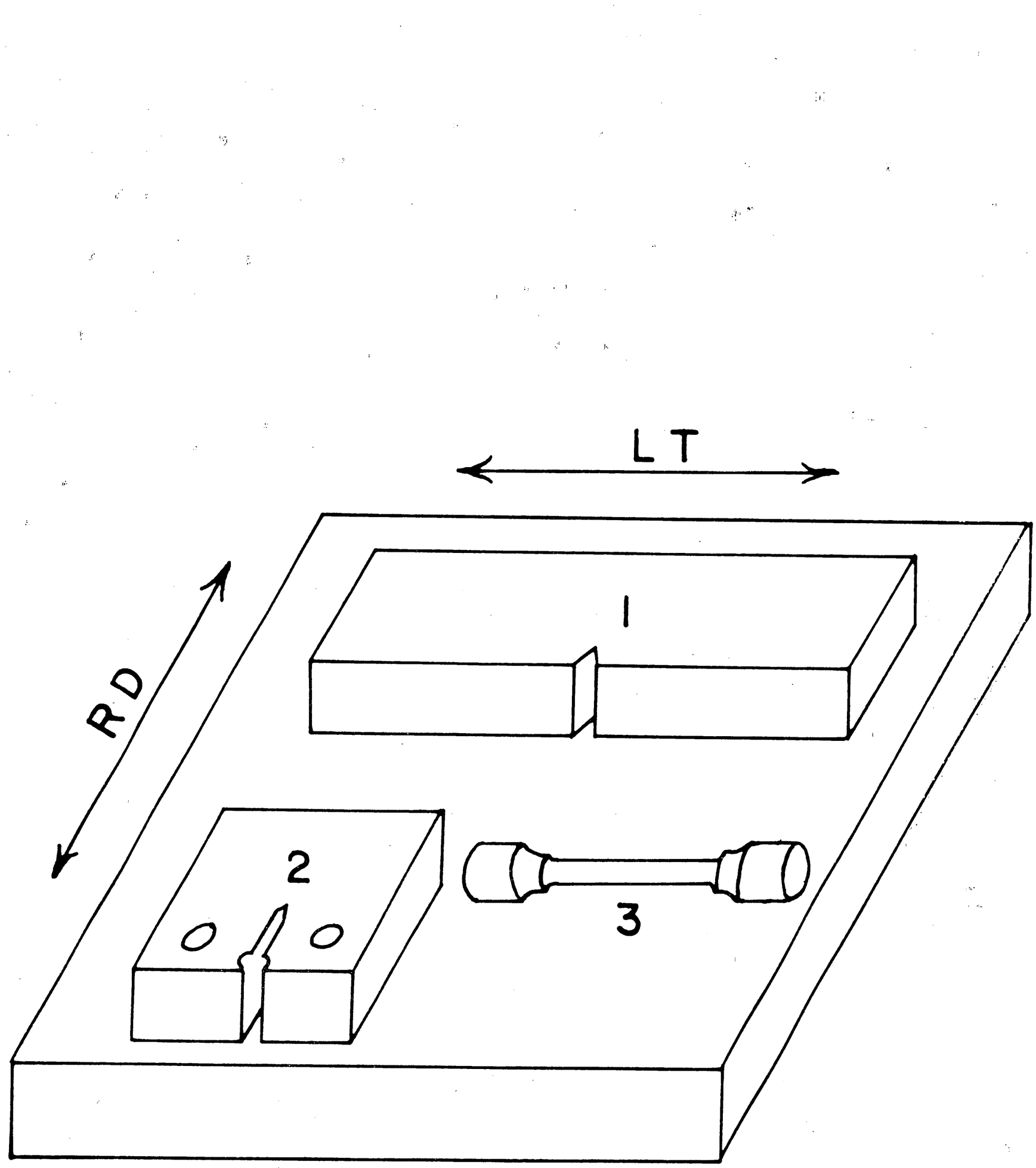

1 1 IN. DT - K_{ID}

2 COMPACT TENSION K_{IC}

3 TRANSVERSE TENSILE

Figure 8 — [illegible] Specimen Orientation

TEST PROGRAM

Schedule

Each of the eighteen 1 in. DT specimens was subjected to a combined DT-K_{1D} test. One half of the broken specimen from this test was cut into two compact tension (K_{1C}) and two tensile blanks which were subsequently machined and tested. The manner in which the compact tension and tensile specimens were cut from the broken half of the DT-K_{1D} specimen is shown in Figure 9. All tests were conducted at room temperature.

In addition to the major test program, tensile tests at various strain rates were conducted in order to determine the sensitivity of the alloy's yield strength to rate of loading.

Combined 1 in. DT-K_{1D} Test

Standards for the 1 in. Dynamic Tear test have been promulgated by the Naval Research Laboratory (NRL).[31] While no standards exist for dynamic plane strain fracture toughness testing, what appears to be an acceptable procedure has been established at the Fritz Engineering Laboratory, Lehigh University.[11] The two tests have very much in common, both consisting primarily of impacting a simply supported beam type specimen having a crack starter notch on the tension side. From each test a load versus time oscilloscope trace is used for calculation of the test result. In the DT test a calibrated energy absorption

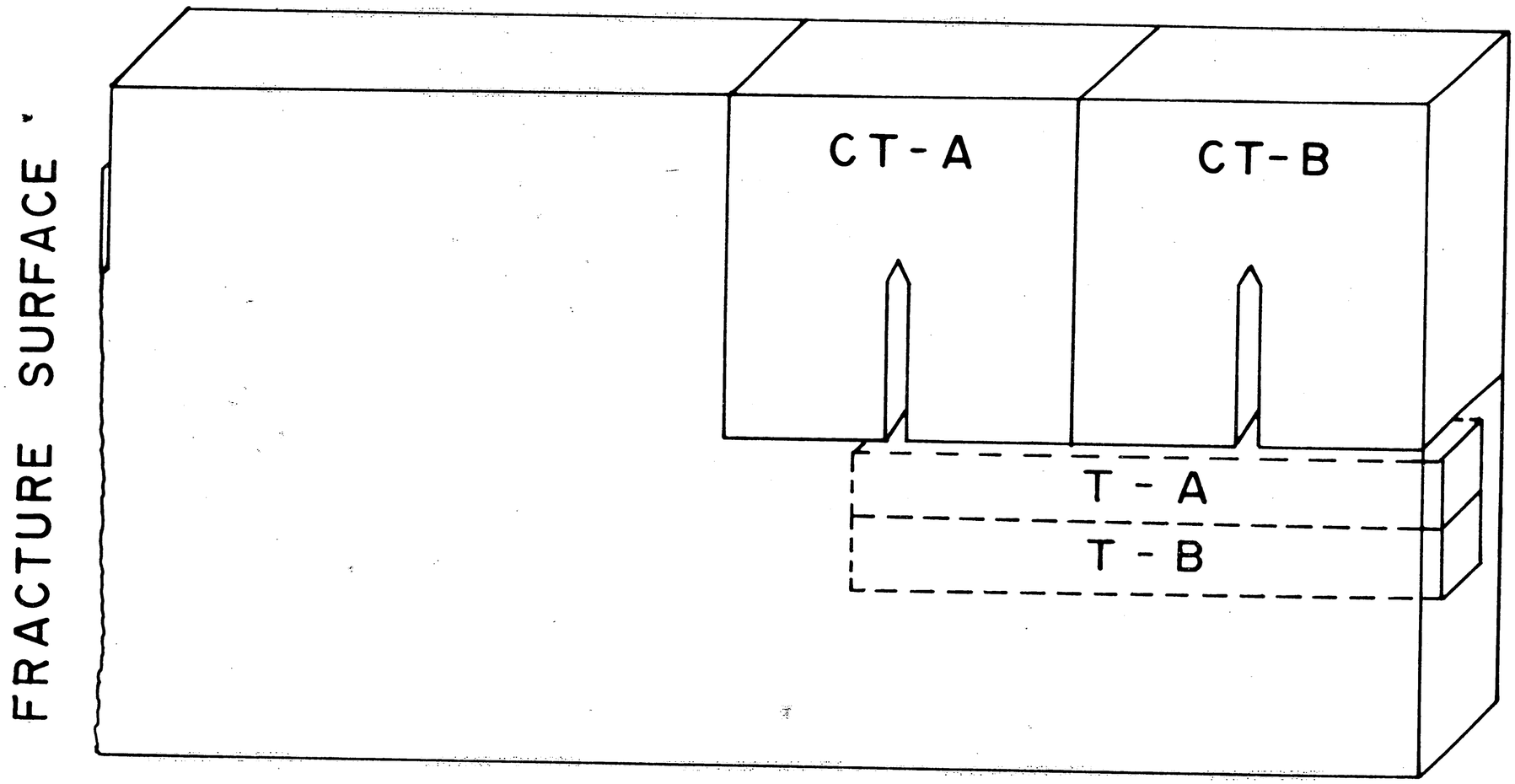

Figure 9 — Layout of Compact Tension and Tensile Specimen Removal from Fractured Half of 1-in. DT-K_{ID} Specimen

system may be used as an alternate method for the determination of the test result.

The DT-K_{ID} specimen geometry is shown in Figure 10. Table V defines the symbols and indicates the dimensions of each. The specimen

Symbol	Parameter	Dimension
B	Thickness	1 in.
W	Width	4.75 in.
L	Length	18.0 in.
a	Crack Length	1.75 in. nom.
W-a	Ligament Length	3.0 in.
S	Span Length	16.0 in.

Table V — Symbol Description and Specimen Dimensions for Combined DT-K_{ID} Test

was somewhat larger than that normally used at Fritz Engineering Laboratory for K_{ID} testing, but it had the same ratios of S/W and a/W.

Two major differences between the DT and K_{ID} tests are drop height and the nature of the crack starter notch. NRL specifies a 4 ft. to 7 ft. drop height to insure the maximum strain rate effect. Strain rate is a test variable in the K_{ID} test and drop heights of as low as 1 ft. are commonly used. The crack starter notch for the K_{ID} test is a fatigue pre-crack chevron notch while that of the DT test is a brittle electron beam weld which is supposedly equivalent under dynamic loading conditions.[8, 32] The crack starter notch for the combined DT-K_{ID} test was a chevron V-notch which was pre-cracked to a depth at which the remaining ligament had a nominal length of 3 in. An illustration of

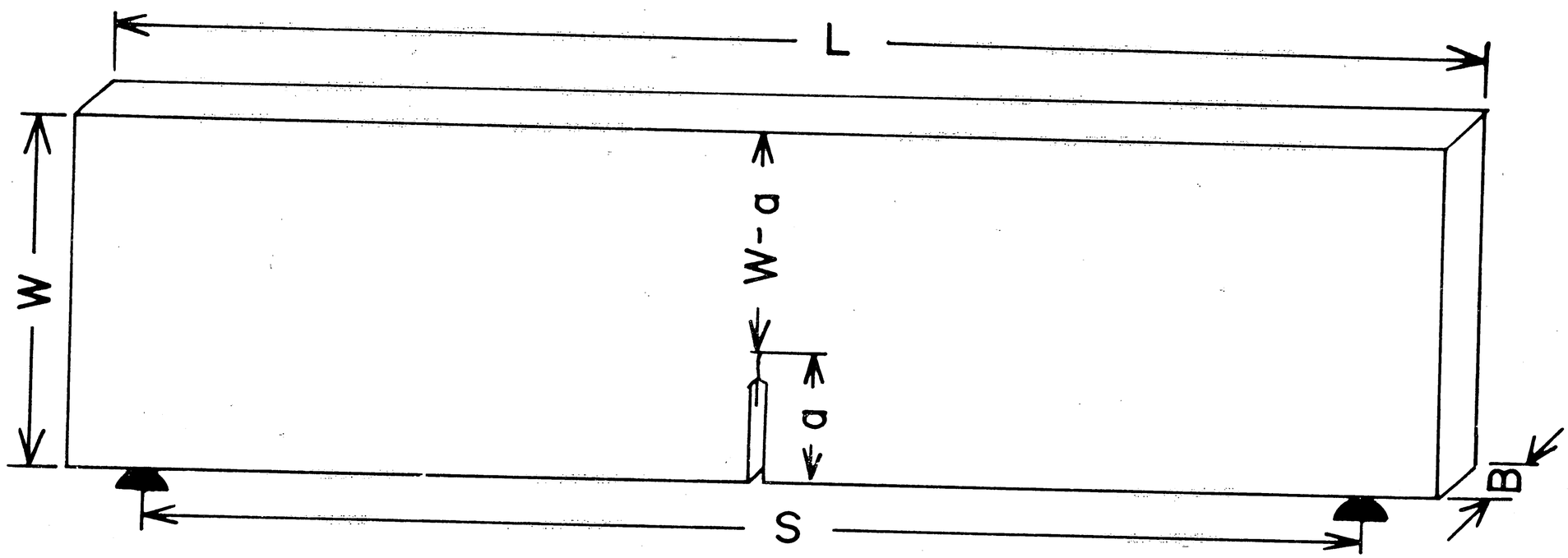

Figure 10 — 1-in. DT K_{ID} Specimen Geometry

the fracture plane depicting this configuration is shown in Figure 11.

Pre-cracking was done on a 10 ton capacity Amsler High Frequency Vibraphore at maximum loads of less than 50% of the loads expected for fracture. The final 6% of the crack length was fatigue pre-cracked at loads of less than 30% of those expected for fracture. This reduction of maximum load during pre-cracking was intended to reduce strain hardening effects in the vicinity of the crack tip and accounts for the two fatigue zones shown in Figure 11.

The pre-cracked bend specimens were tested using the drop weight testing machine shown in Figure 12. This machine featured a 400 lb. weight which was allowed to free fall by the actuation of an electromagnetic release mechanism. The weight was equipped with an instrumented tup from which loads were recorded during testing. The testing arrangement is shown in Figure 13. The loading cushions shown in this figure were used to spread out the loading time and reduce inertial effects which have been shown to obscure the actual test record. These cushions, made of ½ in. drill rod, are not used in the standard DT test as prescribed by NRL. The aluminum blocks shown in Figure 13 served as the calibrated energy absorption system previously mentioned as an alternative method for the determination of DT energy.

When a test was conducted, a photoelectric cell actuated by the falling weight triggered a Taktronix Type 549 storage oscilloscope into which the signal from the load dynamometer (instrumented tup) was transferred. This resulted in a continuous load-time trace on the oscilloscope screen, a photograph of which served as the test record.

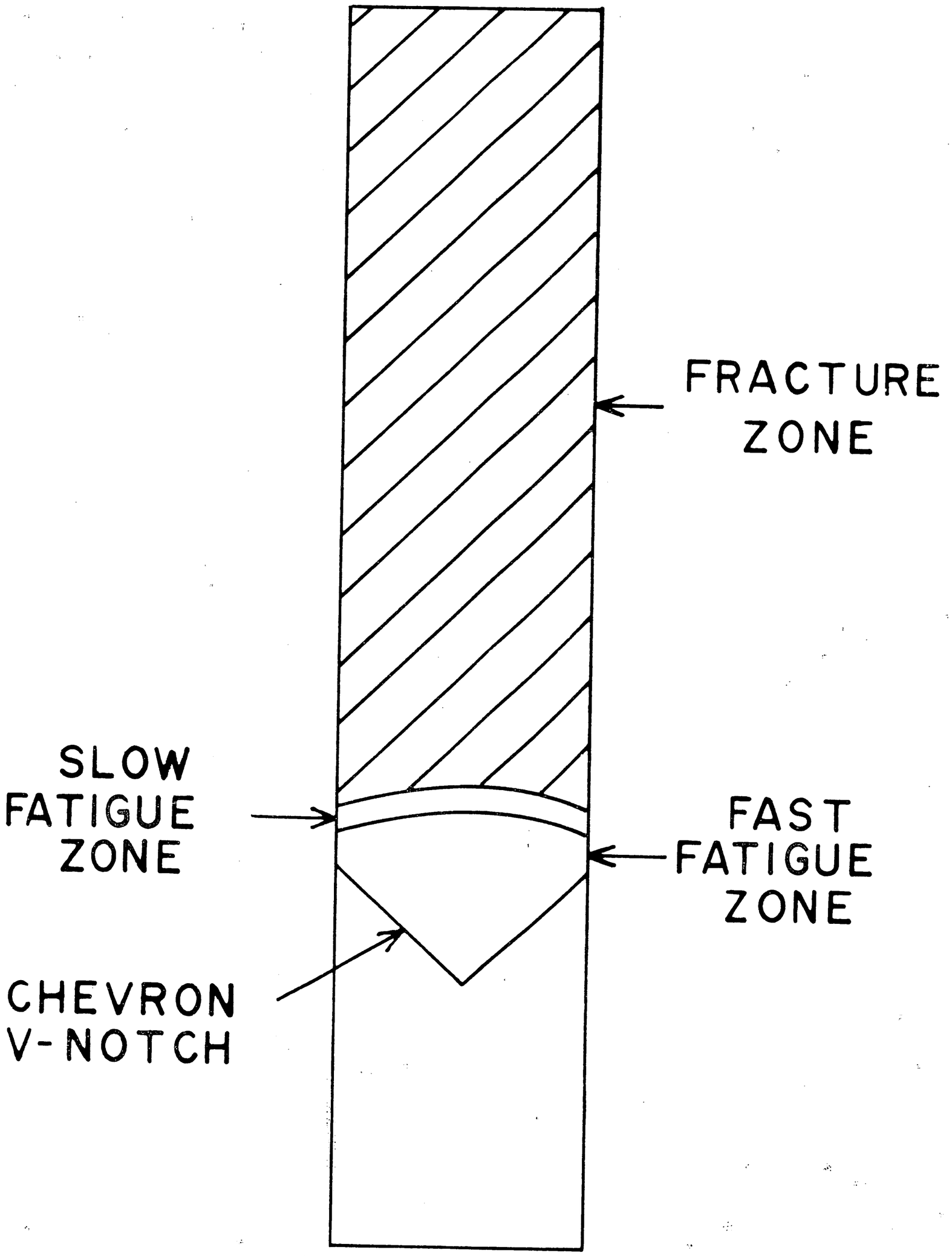

Figure 11 -- Crack Starter Configuration
for 1-in. DT-K Specimen

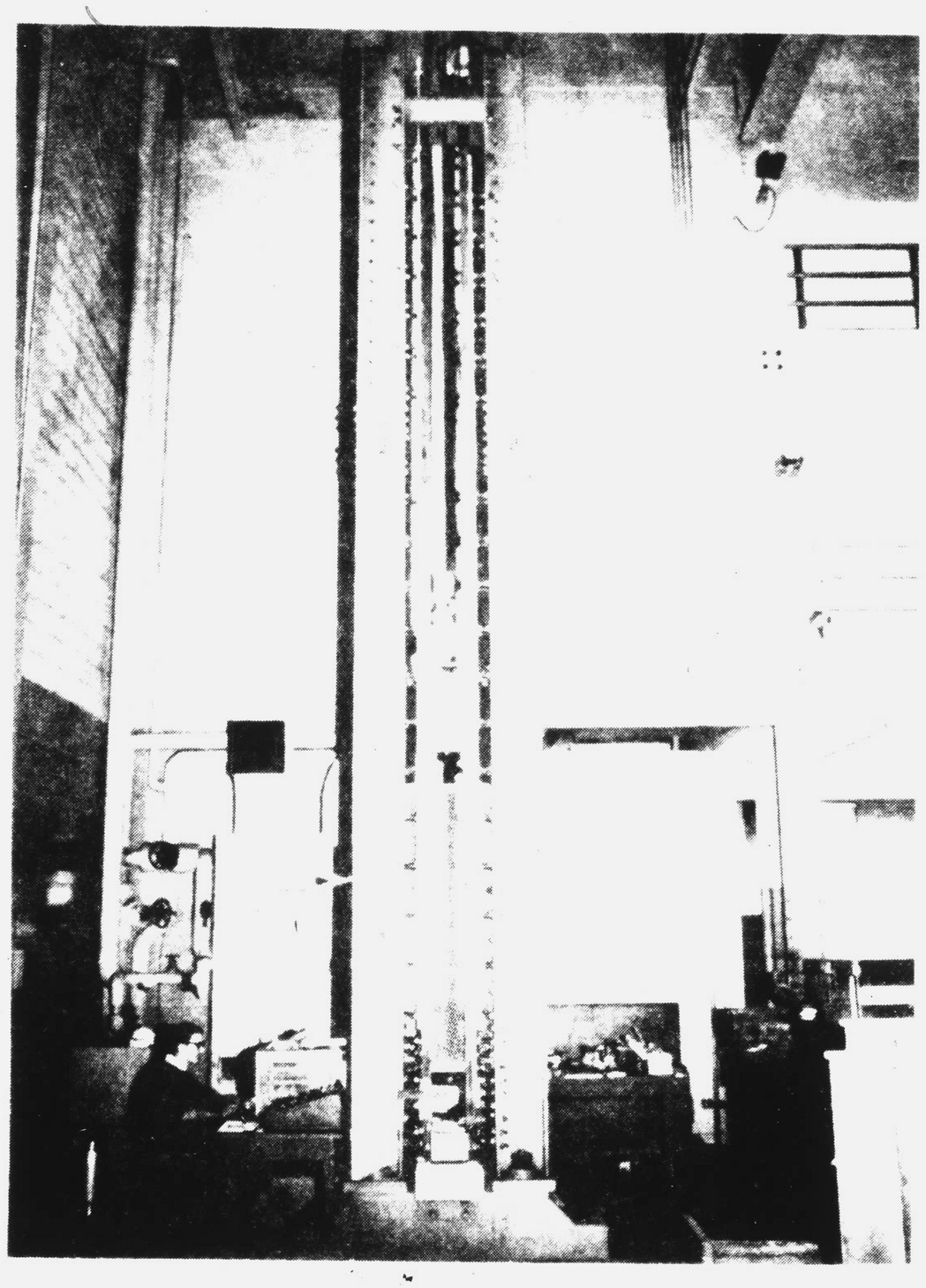

Figure 12 — Drop Weight Testing Machine

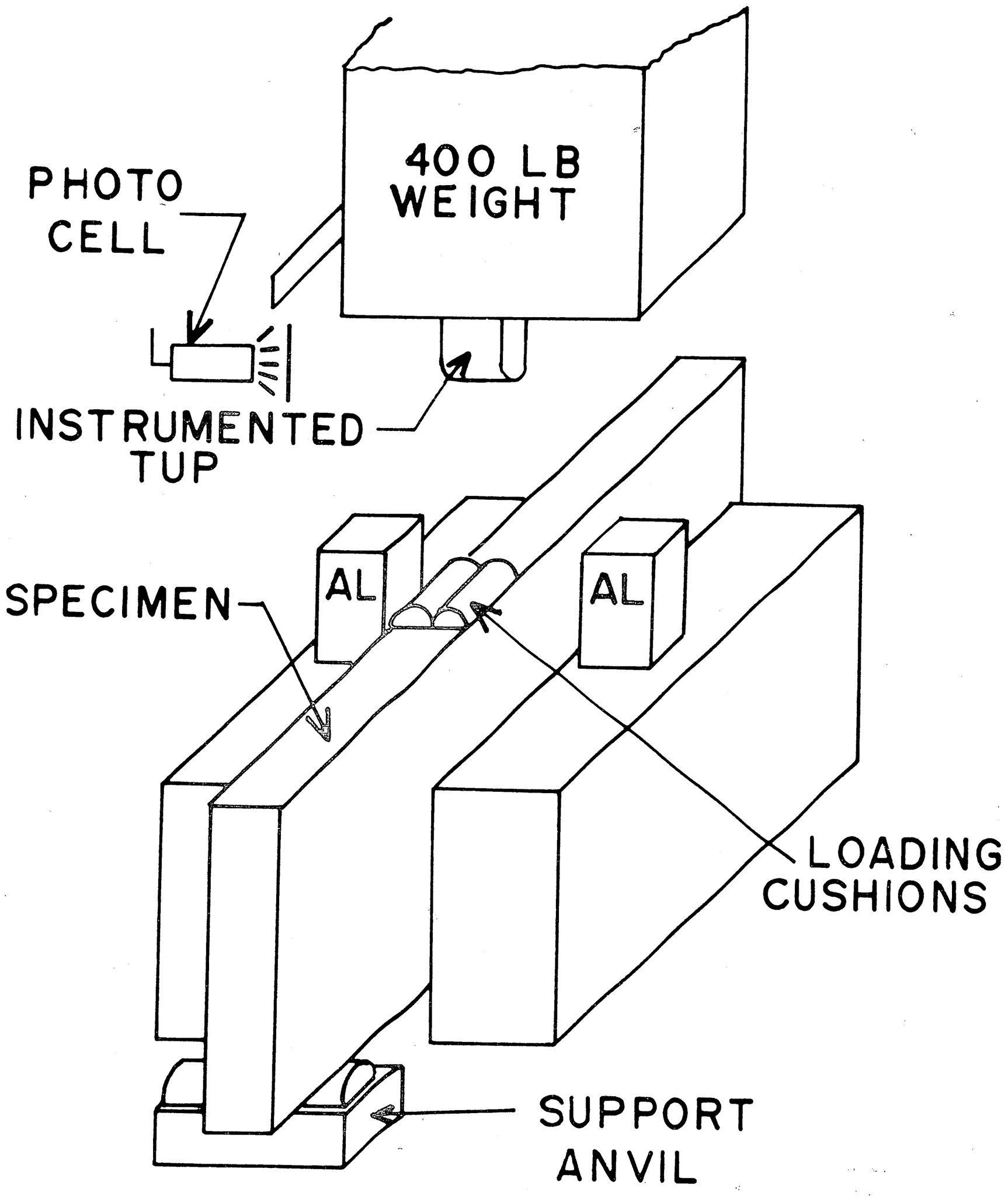

Figure 13 — Test Arrangement for 1-in. DT-K_{ID} Tests

Kinetic energy remaining after fracture of the specimen was absorbed by compression of the aluminum blocks, for which an energy absorption calibration curve had been developed.

K_{1C} Test

Static plane strain fracture toughness tests were conducted in accordance with the procedures proposed by the ASTM E-24 committee.[20] A compact tension specimen configuration was used, as was a double cantilever clip-in displacement gage. Figure 14 illustrates the specimen geometry and dimensions. The displacement gage used and the method of mounting is shown in Figure 15. The specimens were chevron V-notched and pre-cracked in a manner similar to that described for the combined 1 in. DT K_{1D} specimens. The tests were conducted on a 120,000 pound Baldwin Universal Testing Machine using loading rates of 5000 to 10,000 lb/min.

Tensile Tests

Tensile tests were conducted with a 10,000 pound capacity Instron Testing Machine using shouldered 4 in. long specimens with a 1 in. gage length and 0.250 in. nominal diameter. A cross-head speed of 0.05 in/min. was used, corresponding to a nominal strain rate of 10^{-3} sec^{-1}. An Instron Type G 51-12 strain gage extensometer was used until after yielding occurred. A load-extensometer record was obtained for each test.

The strain rate sensitivity tests were conducted with cross-head speeds of 0.002 to 2.0 in/min. corresponding to strain rates of

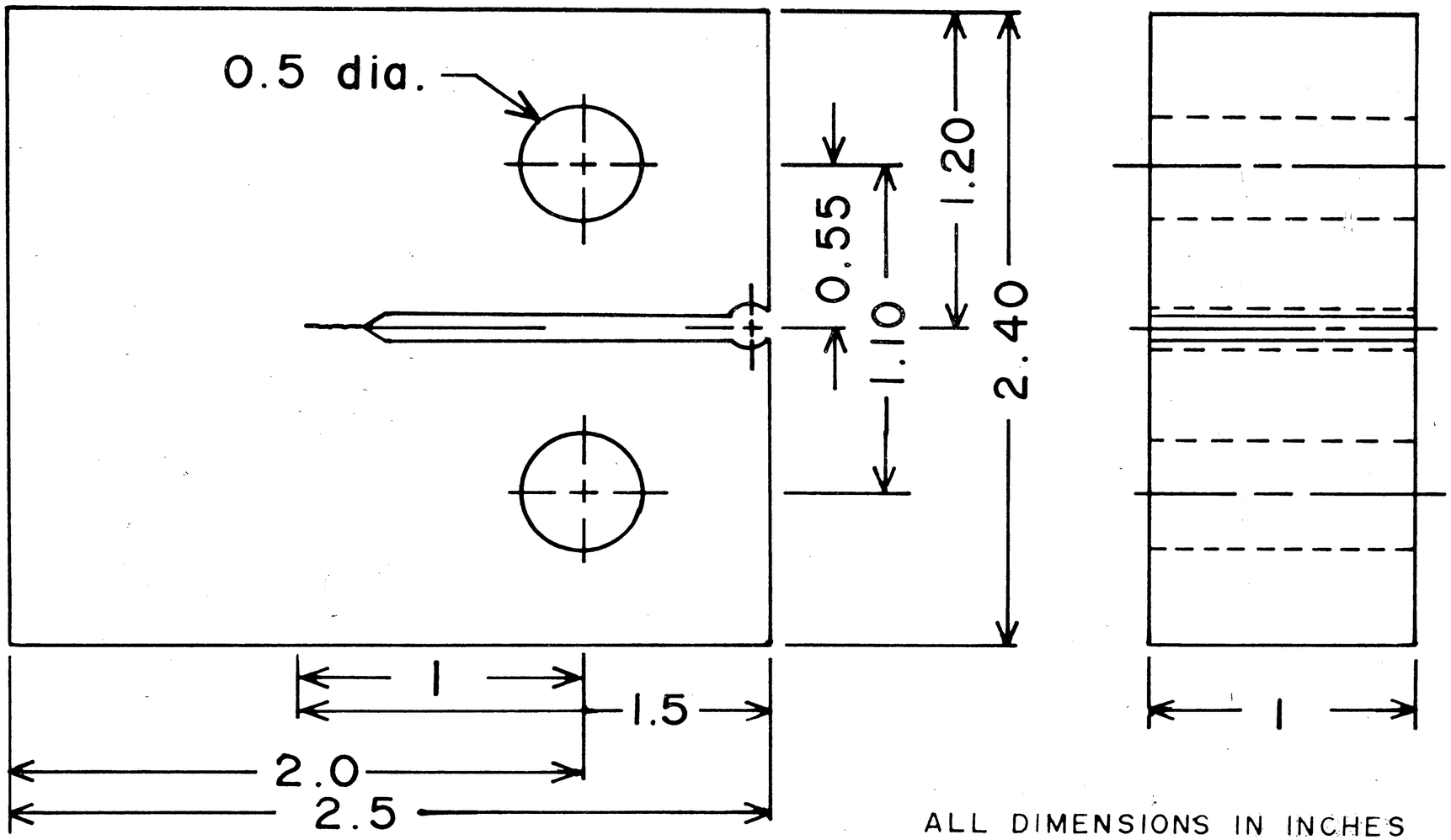

Figure 14 — Compact Tension K_{IC} Specimen

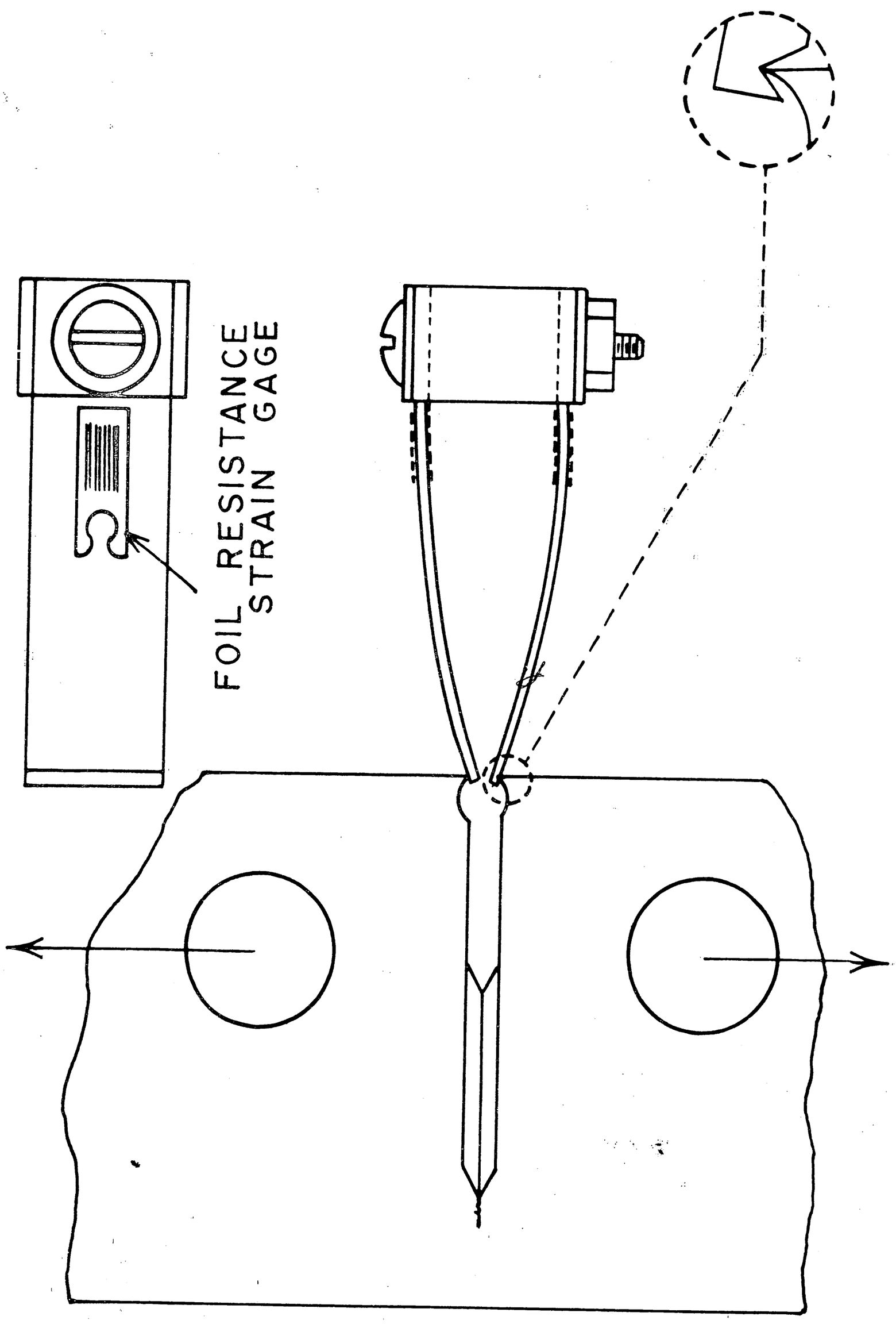

Figure 1. — Displacement Gage and Method of Mounting

2×10^{-5} to 2×10^{-2} sec^{-1}. The specimens used were similar to those described above except that their gage diameter was reduced to approximately 0.12 in. so that the capacity of the Instron would not be exceeded at the high strain rates. Likewise, an extensometer was not used because rapid fracture was expected at the high strain rates. The test record consisted of a load-displacement record based on chart and cross-head speed. It was assumed that the full 1.75 in. reduced section underwent uniform elongation before yielding occurred. Though approximate, this assumption was considered suitable for the purposes of these tests.

SPECIMEN ANALYSIS

Dynamic Plane Strain Fracture Toughness

The dynamic plane strain fracture toughness was calculated using the following expression:[11]

$$K_{QD} = \frac{1.5PS(a)^{\frac{1}{2}}}{BW^2} Y \tag{5}$$

where a = crack length, in.

B = thickness, in.

W = depth, in.

P = maximum load recorded on load-time trace, lbs.

S = span length, in.

Y = $f(a/W)$ given by the following power series for $S/W = 3.33$

$$Y = 1.93 - 3.12(a/W) + 14.68(a/W)^2 - 25.3(a/W)^3 + 25.9(a/W)^4 \tag{6}$$

A plastic zone correction was applied to account for the fact that the crack length is effectively lenghtned by plastic yielding in front of the crack tip. The plastic zone size (r_p) is given by the expression:

$$r_p = \frac{1}{2\pi}\left(\frac{K_{QD}}{\sigma_{YD}}\right)^2 \tag{7}$$

where K_{QD} is determined from equation (5) and σ_{YD} is the dynamic yield strength. The corrected crack length (a_1) is then:

$$a_1 = a + r_p \tag{8}$$

A corrected K_{QD} is then calculated with equation (5) using a_1 and its corresponding Y function.

In accordance with the procedures used in reference 11, a plasticity correction is then applied to the corrected K_{QD} to arrive at K_{1D}. K_{QD} is related to K_{1D} by the expression:

$$K_{1D}^2 = \frac{K_{QD}^2}{1 + .5\beta} \tag{9}$$

where β is a dimensionless parameter determined by:

$$\beta = \frac{1}{B}\left(\frac{K_{QD}}{\sigma_{YD}}\right)^2 \tag{10}$$

A sample calculation of K_{1D} is shown in Appendix A.

Dynamic Tear Energy

Dynamic tear energy was determined from the same test as the dynamic plane strain fracture toughness. Two methods were used to determine DT energy, both of which are recommended by NRL. The first and most simple was an energy summation method using the calibrated energy absorption system. The energy absorbed in fracture of the specimen (DT_U) was determined by:

$$DT_U = U_T - U_C - U_B \tag{11}$$

where U_T = total energy applied, ft-lbs

U_C = energy absorbed by loading cushions, ft-lbs

U_B = energy absorbed by aluminum blocks, ft-lbs

U_T was determined from the potential energy of the weight before it was released and is simply the product of the weight and the drop height.

Energy absorbed in the loading cushions and aluminum blocks was determined from calibration curves developed by a co-worker conducting similar tests on bridge steels. In the case of the loading cushions it was found that energy absorption could be correlated to the length of the region deformed by the striking tup. This correlation is shown in Figure 16. For the aluminum blocks, it was determined that the energy absorbed could be correlated with the amount of compressive deformation as measured by the change in block height. This correlation is shown in Figure 17.

The second method for the determination of DT energy was by use of the area under the load-time trace. This area represents impulse (I) which is related to DT by:

$$DT_I = I\left(v - \frac{I}{2m}\right) \tag{12}$$

where I = impulse, lb-sec

v = tup velocity, ft/sec

m = mass of drop weight, lbm

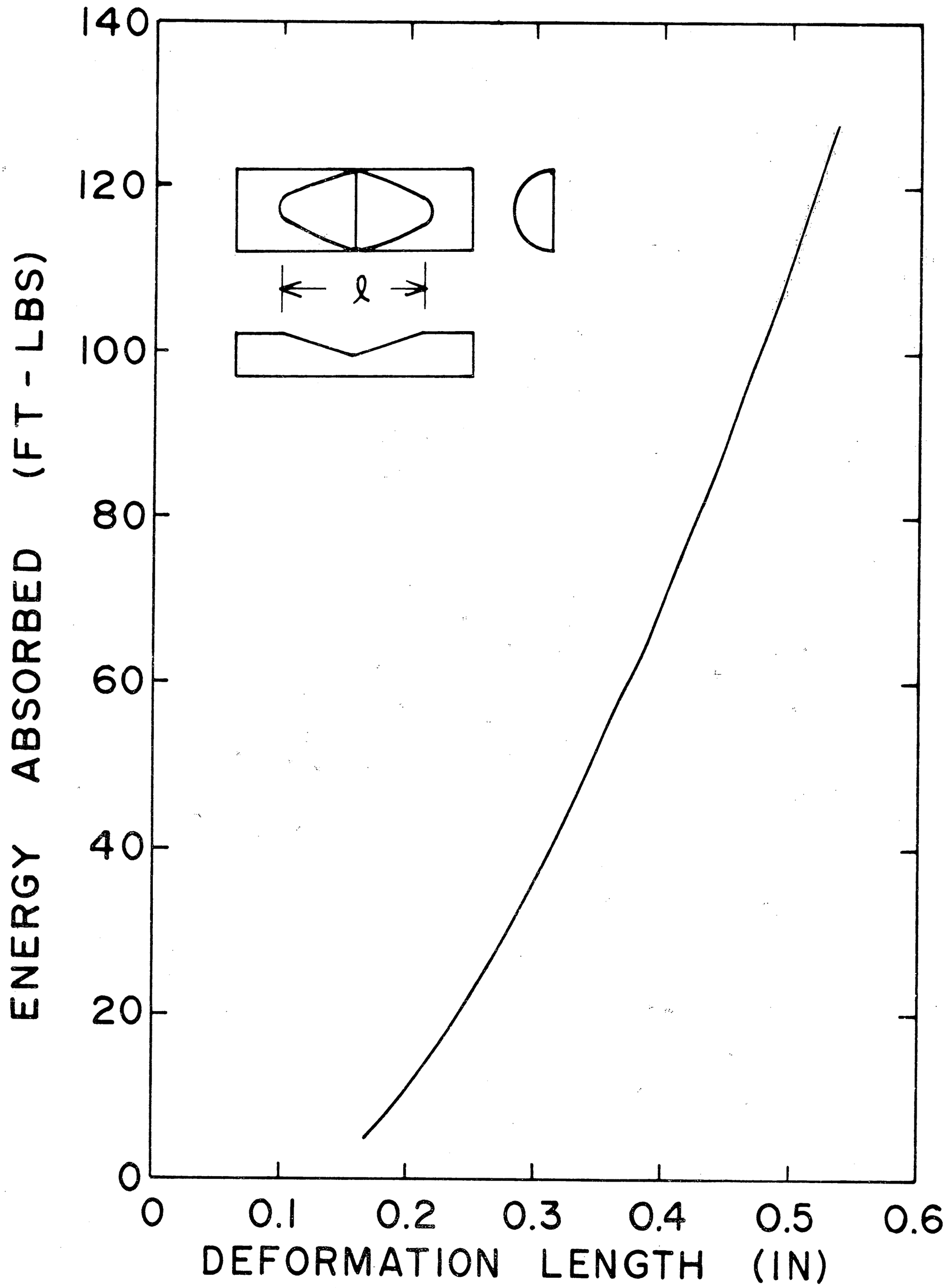

Figure 16 — Calibration Curve for
Energy Absorption of Loading Cushions

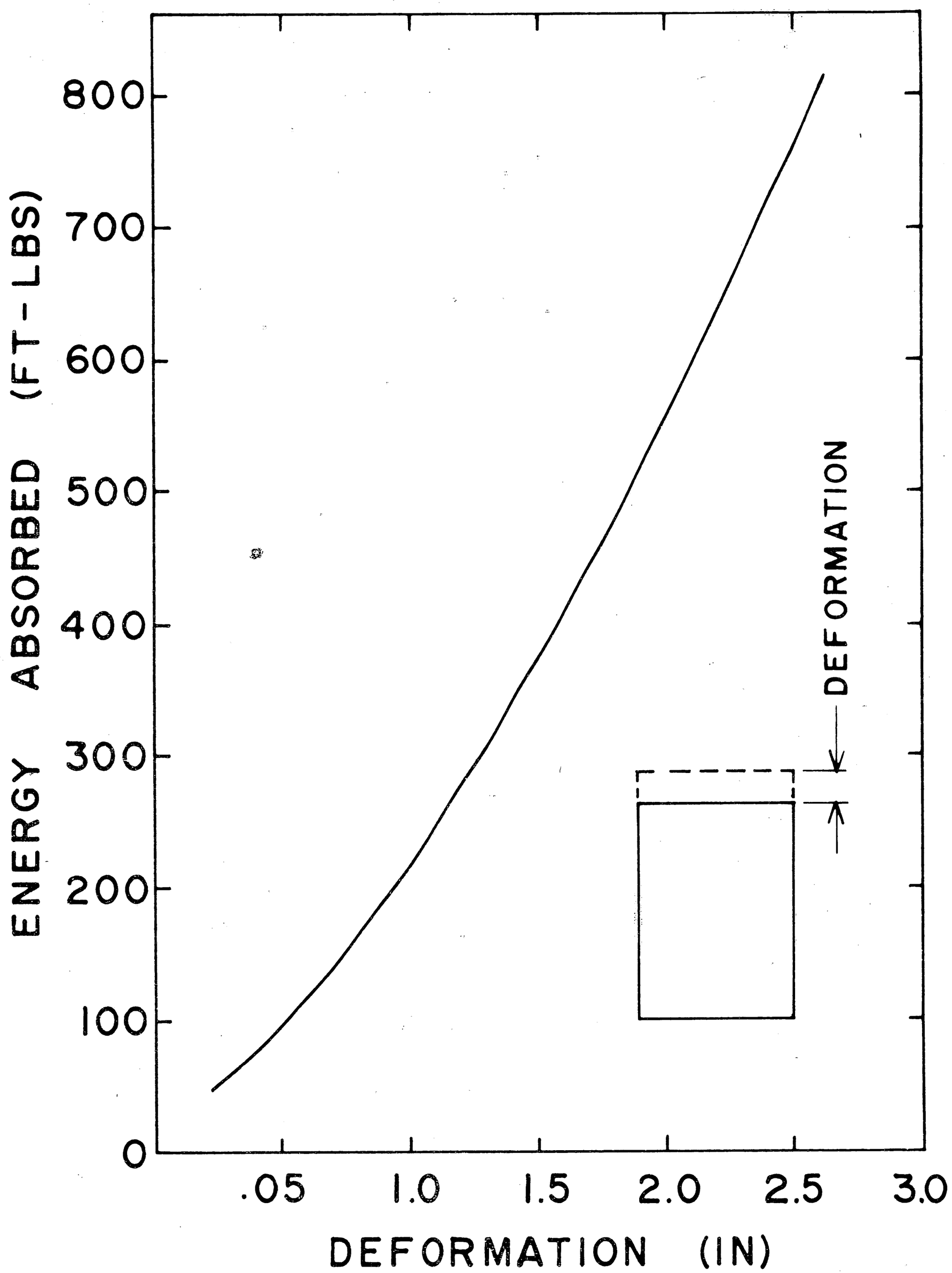

Figure 17 — Calibration Curve for
Energy Absorption of Aluminum Blocks

This equation is developed in Appendix B. The velocity used in equation (12) must reflect the fact that some of the kinetic energy of the falling weight is expended in deforming the loading cushions. The velocity is thus determined by:

$$v = \frac{2}{m}(U_T - U_C) \tag{13}$$

Static Plane Strain Fracture Toughness

The static plane strain fracture toughness was calculated using the expression:[20]

$$K_{QS} = \frac{P_{QS}}{BW^{\frac{1}{2}}} Y' \tag{14}$$

where P = load at 5% secant offset, lbs

B = thickness, in.

W = depth, in.

a = crack length, in.

Y' = $f(a/W)$ given the following power series:

$$Y' = 129.6(a/W)^{1/2} - 185.5(a/W)^{3/2} + 655.7(a/W)^{5/2} - 1017.0(a/W)^{7/2} + 638.9(a/W)^{9/2} \tag{15}$$

The validity of the K_{QS} value calculated from equation (14) was based on the following criteria:

$$a \geq 2.5\left(\frac{K_{QS}}{\sigma_{YS}}\right)^2 \tag{16}$$

$$B \geq 2.5 \left(\frac{K_{QS}}{\sigma_{YS}}\right)^2 \tag{17}$$

$$W-a \geq 2.5 \left(\frac{K_{QS}}{\sigma_{YS}}\right)^2 \tag{18}$$

where σ_{YS} was the static yield strength. Significant deviation from the other validity requirements set forth by the ASTM E-24 committee will be discussed individually where applicable. For purposes of graphical comparisons involving K_{1C} and K_{1D}, plastic zone size and beta corrections were applied to K_{1C} using equations similar to equations (7) through (10). This was to insure uniformity in analysis.

TEST RESULTS

Tensile Tests

The tensile test results are shown in Table VI. Tensile tests were not conducted on specimens 4, 8, or 12. The test results point

Group No.	Spec. No.	Yield Strength (ksi)		Tensile Strength (ksi)		Elastic Modulus (10^6 psi)	
		A	B	A	B	A	B
I	1	131.9	138.0	155.3	158.9	14.82	13.14
	2	147.5	147.7	165.7	165.0	16.96	19.96
	3	143.7	143.6	170.4	166.5	15.97	16.70
II	5	152.1	148.3	163.5	157.4	18.55	19.26
	6	145.0	143.2	154.4	153.0	17.69	19.36
	7	138.5	139.5	148.7	147.0	18.23	19.65
III	9	149.5	147.6	161.5	161.5	17.59	18.22
	10	160.2	156.9	171.8	165.4	19.07	16.87
	11	150.4	149.5	158.4	157.3	19.53	18.92
IV	13	162.9	161.2	175.1	173.3	16.83	15.87
	14		161.9		173.2		16.19
	15	147.7	146.8	169.1	166.1	18.23	13.98
V	16		148.0		155.3		20.8
	17		157.3		164.8		21.26
	18	153.6	154.0	158.9	160.2	18.51	19.49

Table VI — Tensile Test Results

out several important characteristics of the test material. Most notable is the inconsistent response to heat treatment. This is most apparent in Groups I, II, and IV where variation in yield strength within each group is as much as 16 ksi. It is doubtful that this is

the result of variation in test procedures since the A and B tensile specimen from each DT-K_{1D} plate had almost identical results in every group. All three plates of Group I had yield strengths significantly higher than that obtained during preliminary testing of specimens with ½-in. square cross-section (Table III). This evidently represents the inability of the test material to respond well to solution treatment in thick sections. Recent work by NRL indicates a similar response.[12] Variation of yield strength in Groups II and IV also can probably be attributed to solution treatment response.

The variation in the elastic modulus between groups is another important characteristic brought out by the tensile tests. The elastic modulus of titanium alloys is commonly taken as 16×10^6 psi. Table VI indicates a variation from 14×10^6 psi to 21×10^6 psi in elastic modulus. Similar variation has been reported previously[25] but is not generally considered. The variation becomes significant when applied to equation (1), (3), or (4). For example, K_{1D}^2/E for the Group V specimens would be 20% in error if an elastic modulus of 16×10^6 psi were used. It may also be observed that within each group (except Group I) the variation in elastic modulus is small. Group IV, which had the largest variation in yield strength has the least variation in elastic modulus.

Strain Rate Sensitivity Tests

The results of the tensile tests conducted at various strain rates is shown in Table VII. It was apparent that the yield strength of the test material is, in fact, strain rate sensitive. This was expected

since the alloy's yield strength has been shown to be quite sensitive to temperature.[26]

Strain Rate (sec^{-1})	Yield Strength (ksi)	Number of Tests
2×10^{-5}	150.9	2
2×10^{-4}	153.6	3
2×10^{-3}	156.5	2
2×10^{-2}	159.0	5

Table VII — Results of Strain Rate Sensitivity Tensile Tests

Static Plane Strain Fracture Toughness

The static plane strain fracture toughness (K_{1C}) test results are shown in Table VIII. All of the test results were valid based on equations (16), (17), and (18). The Group I and IV results were technically invalid because the surface trace of the crack was less than 90% of the crack length (a). The small radius of curvature of the crack front of these two groups may be associated with the fact that they also had the lowest elastic moduli. The only other ASTM criteria for validity which was exceeded was the maximum stress intensity level during the final stage of pre-cracking of specimens 3 and 10. $K_{f(max)}$ for these specimens was 0.65 and 0.75 of their respective K_Q value. The limit for valid K_{1C} values is 0.60.

As in the tensile test results, a variation of K_{1C} within each group was observed but similar values were obtained for the A and B specimens cut from the same DT-K_{1D} plate. The effect of overageing

Group No.	Spec. No.	K_{1C} (ksi-$in^{\frac{1}{2}}$)		
		A	B	Average
I	1	77.94		77.94
	2	66.81		66.81
	3	63.57	54.94	59.26
II	5	56.64	53.77	55.21
	6		82.13	82.13
	7	83.04	85.47	84.26
III	9	74.05	71.84	73.00
	10	51.89	57.25	54.57
	11	73.40	74.74	74.07
IV	13	55.25	50.82	53.03
	14	53.52	53.66	53.59
	15	65.97	66.59	66.28
V	16	55.42		55.42
	17	41.11	42.78	41.95
	18		43.11	43.11

Table VIII — Static Plane Strain
Fracture Toughness Test Results

the Group V specimens was significant. While equal in yield strength to the Group III specimens, their static plane strain fracture toughness was reduced by 20%. Groups II, III, and IV represent similar heat treatments compared to Groups I and V. Within these three groups a definite trend of decreasing fracture toughness with increasing yield strength was observed.

Dynamic Plane Strain Fracture Toughness

Table IX lists the results of the dynamic plane strain fracture toughness tests. Dynamic fracture toughness levels significantly

Group No.	Spec. No.	K_{1D} (ksi-in$^{\frac{1}{2}}$)
I	1	114.6
	2	119.8
	3	115.6
II	5	119.9
	6	118.6
	7	123.9
III	9	125.0
	10	121.4
	11	116.2
	12	116.4
IV	13	100.4
	14	106.9
V	16	89.9
	17	109.7
	18	96.4

Table IX — Dynamic Plane Strain
Fracture Toughness Test Results

higher than those for the static case were confirmed. Significant variation within each group is again observed. Values for specimens 4, 8, and 15 were not obtained because of testing difficulties. The storage oscilloscope was very sensitive and was prematurely triggered by the control button for the electro-magnetic release mechanism. The effect of overageing the Group V specimens was apparent in the K_{1D} results as it was in those for K_{1C}. The decreasing trend of K_{1D} in Groups II, III, and IV was not so dramatic as it was for the K_{1C} results.

Although there are no criteria for validity of K_{1D} tests, those specified for K_{1C} testing should be generally applicable. If dynamic

yield strength is substituted for static yield strength in equations (16), (17), and (18), the right side of the equations is 0.7 to 1.3 for the K_{1D} tests, indicating that plane strain conditions were prevalent. This was substantiated by observation of the fracture surfaces which had less than 15% shear lips.

Dynamic Tear Energy

Table X summarizes the dynamic tear energies obtained by both the energy summation and impulse methods. The last column of Table X is a

Group No.	Spec. No.	DT_U (ft-lbs)	DT_I (ft-lbs)	$\frac{DT_U}{DT_I}$
I	1	234		
	2	144	321	.447
	3	176	269	.653
II	5	460	449	1.02
	6	439		
	7	430	422	1.02
III	9	348	389	.893
	10	310	343	.904
	11		362	
	12	310		
IV	13		247	
	14	310	328	.945
V	16	232	254	.913
	17	257		
	18	243		

Table X — Dynamic Tear Test Results

comparison of the two methods on a ratio basis. The ratio is less than one for all except Group II and is consistent within each group.

Group I had the worst comparison, having very low DT energies by the energy summation method. This may be attributed to the fact that large input energies were used in that group and high energy absorption in the aluminum blocks caused deviation from the calibration curve.

DISCUSSION

Strain Rate Sensitivity of Yield Strength

In order to apply plasticity corrections to K_{QD} using equations (7) through (10), it was necessary to approximate with reasonable accuracy the yield strength of the test material at strain rates on the order of 10^2 sec^{-1} to 10^3 sec^{-1}. The results of the strain rate sensitivity tensile tests (Table VII) indicated that sensitivity definitely existed. While several numerical descriptions of strain rate and temperature effects on yield strength are available for steel, a search of the literature failed to reveal such a description for titanium alloys. For lack of a better alternative, the data of Table VII was compared to a numerical description developed by Rosenfield and Hahn for plain carbon steels.[33] As shown in Figure 18, the comparison was quite favorable and it suggested that this numerical description may be applicable to the test material.

Rosenfield and Hahn presumed that because different mechanisms account for plastic deformation at various temperatures and strain rates, it was unreasonable to expect a single numerical description to adequately describe yield strength in the full range of these variables. Consequently, they divided the temperature-strain rate spectrum into the four regions shown in Figure 19 and suggested an equation applicable to each region. The regions of interest in this research were regions I and II for which the following numerical descriptions apply:

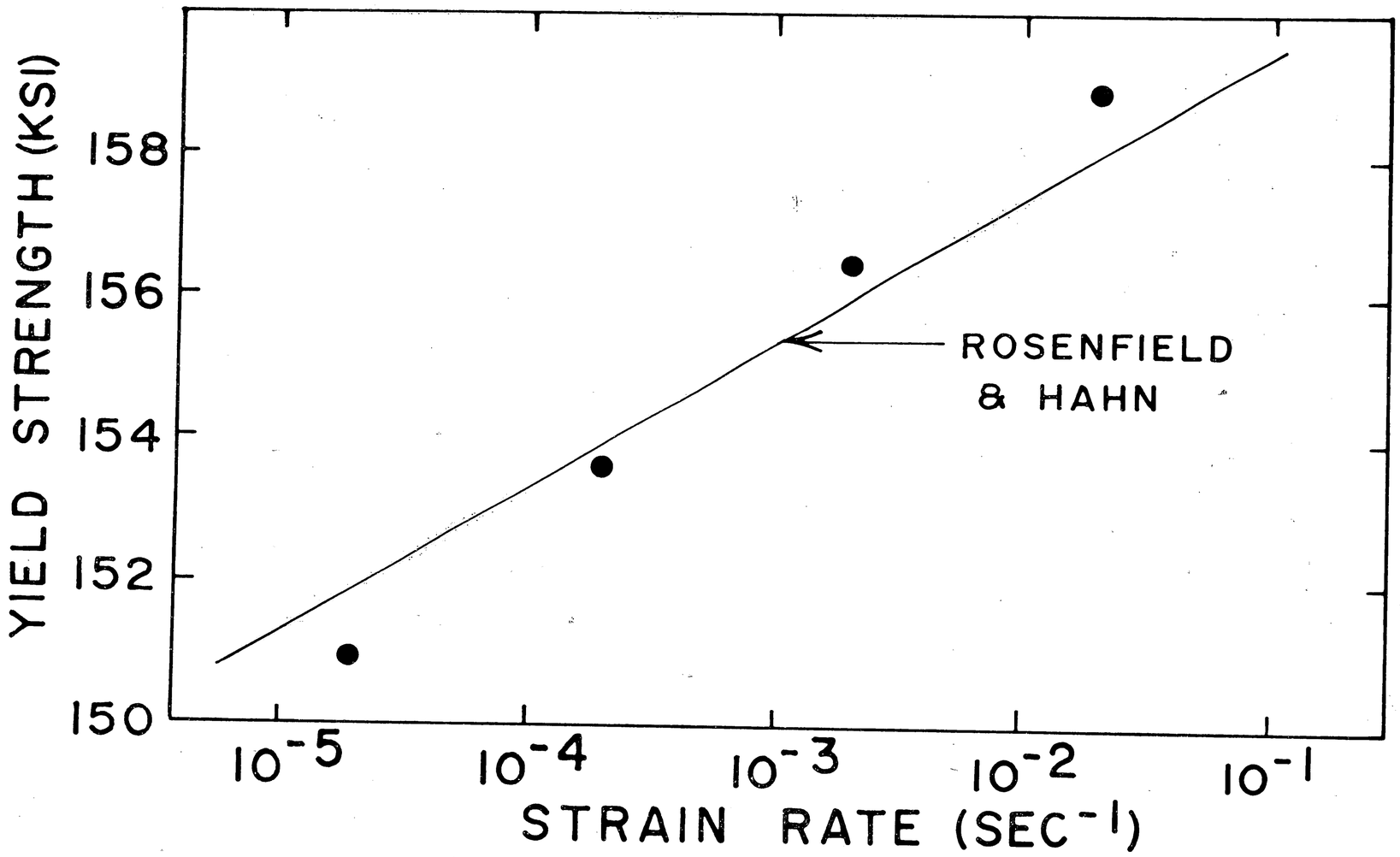

Figure 18 — Comparison of Strain Rate Effect on Yield Strength of Test Material with a Numerical Description of Its Affect on Plain Carbon Steel

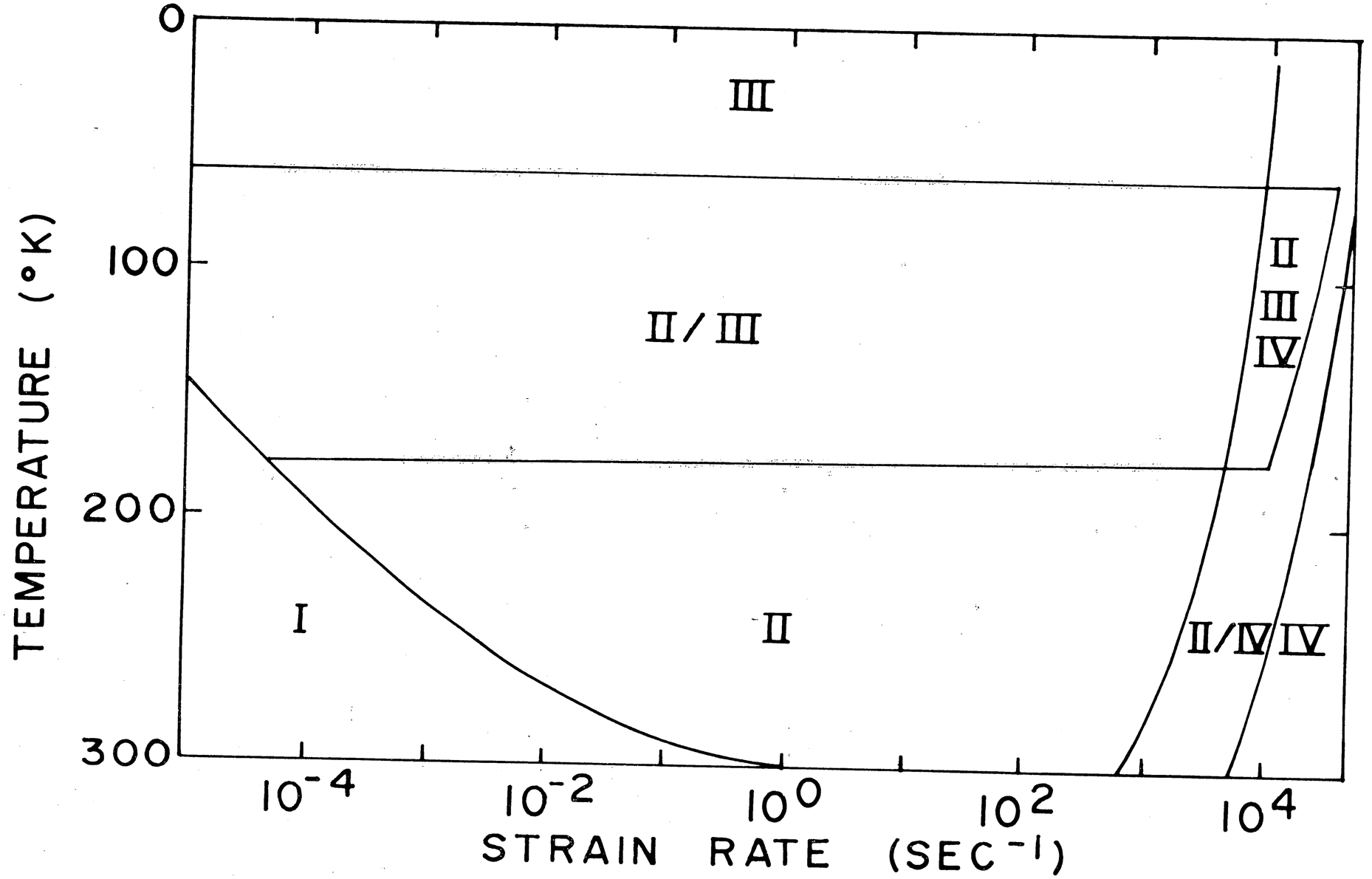

Figure 19 — Temperature-Strain Rate Spectrum (Rosenfield and Hahn)

Region I:

$$\sigma_Y = \sigma_{YS} + 44 - 2.03T^{\frac{1}{2}} + 2 \log \dot{e} \tag{19}$$

Region II:

$$\sigma_Y = \sigma_{YS} + 195 - 11.1T^{\frac{1}{2}} + 8 \log \dot{e} \tag{20}$$

where σ_Y = yield strength at temperature and strain rate of test, ksi

σ_{YS} = yield strength at T = 298°K and $\dot{e} = 10^{-3}$ sec^{-1}, ksi

T = temperature, °K

$\dot{e}$ = strain rate, sec^{-1}

and the transition from region I to region II is determined by:

$$\log \dot{e} \geq 1.39T^{\frac{1}{2}} - 23.7 \tag{21}$$

While the data of Table VII compared well to the equation for region I, it remained to verify the applicability of the equation for region II to the test material since this region included the strain rates associated with dynamic testing. Yield strength data for Ti-6Al-4V covering a wide range of strain rate was found in two sources and is compared with equations (19) and (20) in Figure 20.[34,35] The ordinate axis in this figure was chosen in order to normalize the data since σ_{YS} for each source was slightly different (147 - 154 ksi). Equations (19) and (20) were also applied to low temperature static yield strength data of Vishnevsky and Steigerwald,[26] the results of which are shown in Figure 21. It was apparent from Figures 20 and 21

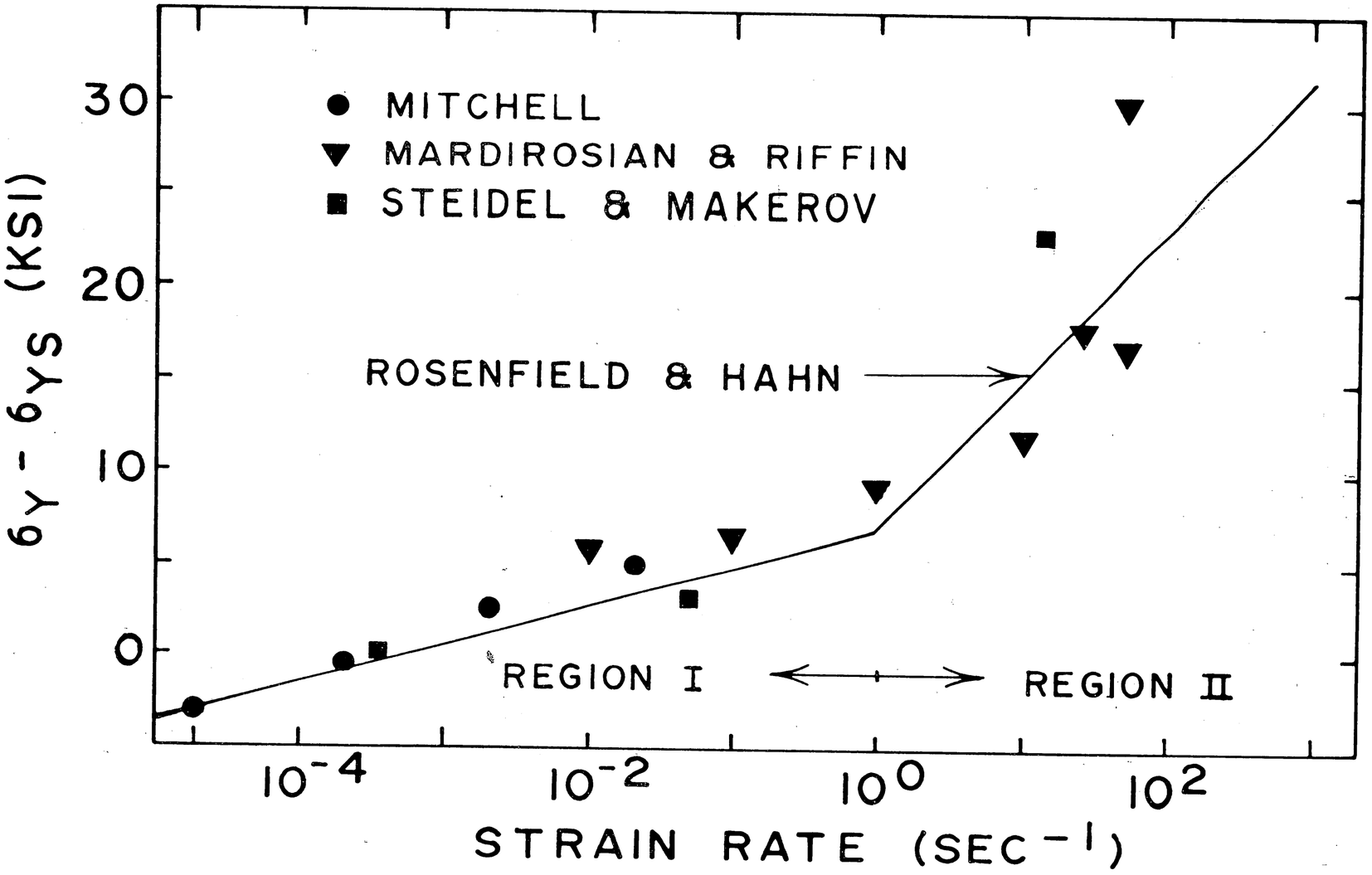

Figure 20 — Strain Rate Effect on Yield Strength of Ti-6Al-4V

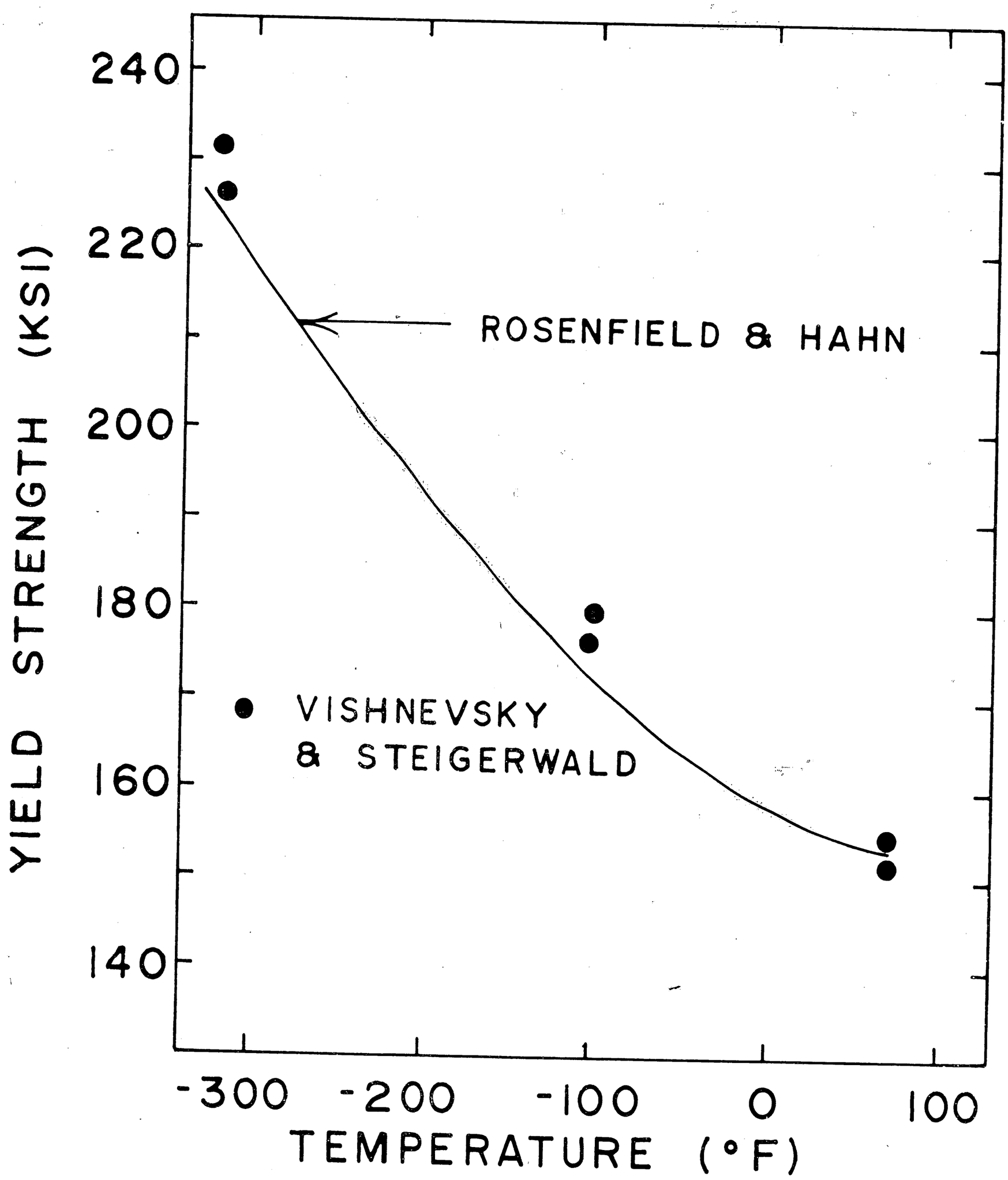

Figure 21 — Comparison of Low Temperature Yield Strength Data with Numerical Description of Rosenfield and Hahn

that the numerical descriptions developed by Rosenfield and Hahn for temperature and strain rate effects on the yield strength of plain carbon steel were also applicable to the test material. Dynamic yield strengths used in equations (7) and (10) were therefore computed using equation (20).

K_{1C} - K_{1D} - DT Correlation

As stated in the introduction and shown in Figure 2, the Naval Research Laboratory has established a reasonable correlation between static plane strain fracture toughness and dynamic tear energy for titanium alloys. Figure 22 is a reproduction of Figure 2, onto which the K_{1C} and DT results of this investigation have been superimposed. In this, as well as the following correlations, the DT energy determined by the impulse method was used except in those cases where it was not obtained. The results have a somewhat larger scatter band than NRL's data, but generally substantiate their correlation. This similarity in results also provides support for the assumption that the EB weld closely simulates the fatigue pre-cracked crackstarter configuration.

As illustrated in Figure 23, the correlation of K_{1D} with DT has the same general trend as K_{1C} with DT. The DT scale has been enlarged in this figure for better portrayal of the region tested. The scatter band is only slightly smaller for the K_{1D} - DT correlation than that for K_{1C} - DT. However, on a relative error basis the K_{1D} - DT correlation is significantly superior, having a maximum relative

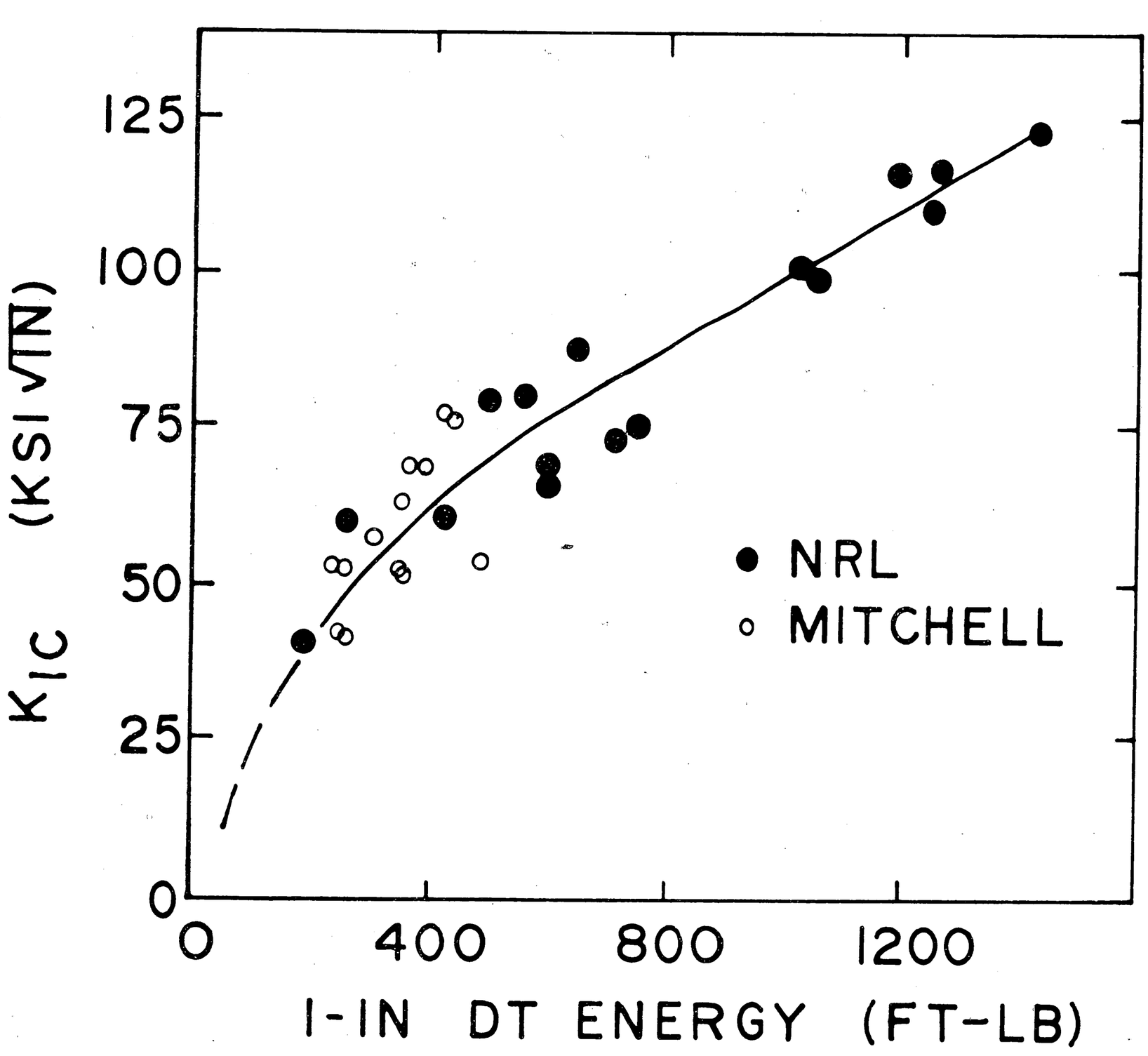

Figure 22 — K_{1C}-DT Correlation

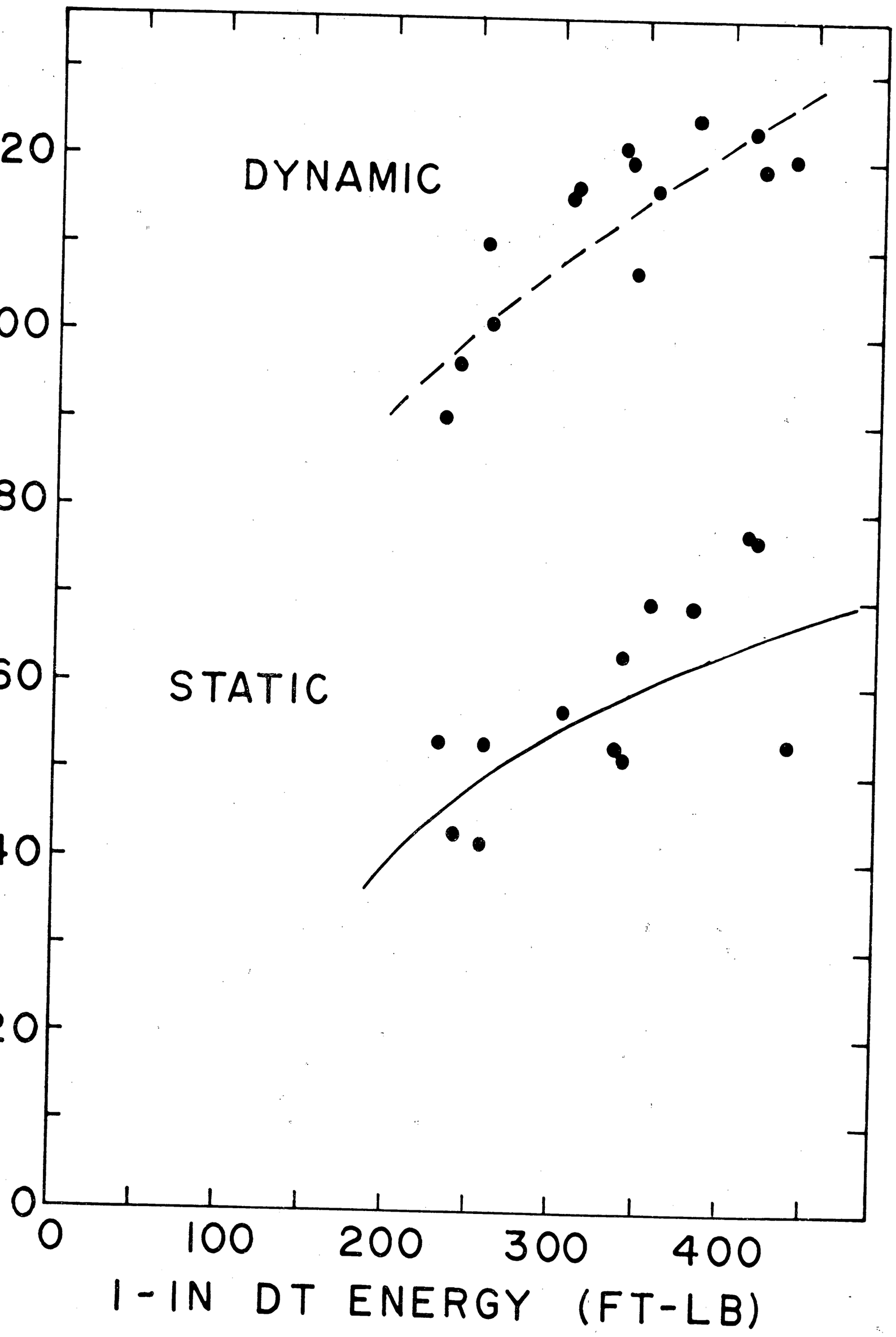

Figure 23 — Correlation of K_{1C} and K_{1D} to DT

error of 9.1% compared to 17% for the K_{1C} - DT correlation. This indicates that for this alloy, K_{1D} could be predicted with almost twice the accuracy of a K_{1C} prediction from DT energy. Additionally, the accuracy of the K_{1D} prediction would be within the 10% variation generally associated with tests of this type.

K_{1C} - K_{1D} - Yield Strength Correlation

The correlation of both dynamic and static plane strain fracture toughness with static yield strength is shown in Figure 24. A general trend of decreasing fracture toughness with increasing yield strength is apparent as is the gross inexactness of the correlations. As an example, for a yield strength of 148 ksi the variation in K_{1D} was 36 ksi-in$^{\frac{1}{2}}$. The K_{1C} - DT correlation had less scatter and a maximum relative error of 19%. This suggests that yield strength is just as suitable for K_{1C} prediction as the DT test for this alloy.

Correlation of Strain Energy Release Rates

The correlation of K_{1D} and DT on the basis of strain energy release rate is shown in Figure 25. Superimposed on this figure is a line representing the equation:

$$\frac{K_{1D}^2}{E}(1-u^2) = \frac{DT}{2A} \qquad (22)$$

where the value of u is taken as 0.37, a value commonly used for titanium alloys although values ranging from 0.287 to 0.42 have been reported.[25,36] The values of K_{1D}^2/E were computed from Tables VI and IX.

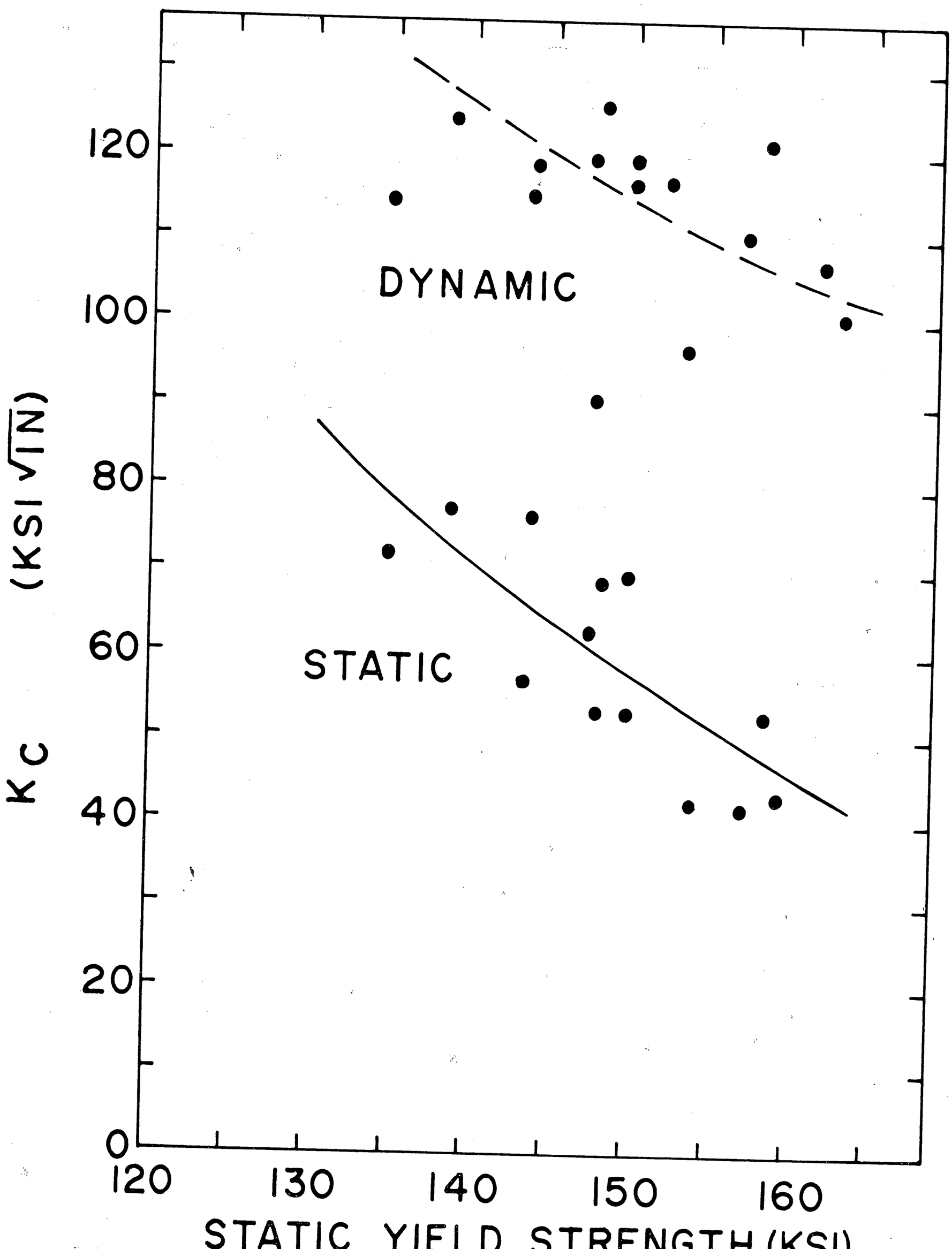

Figure 24 — Correlation of K_{IC} and K_{ID} to Yield Strength

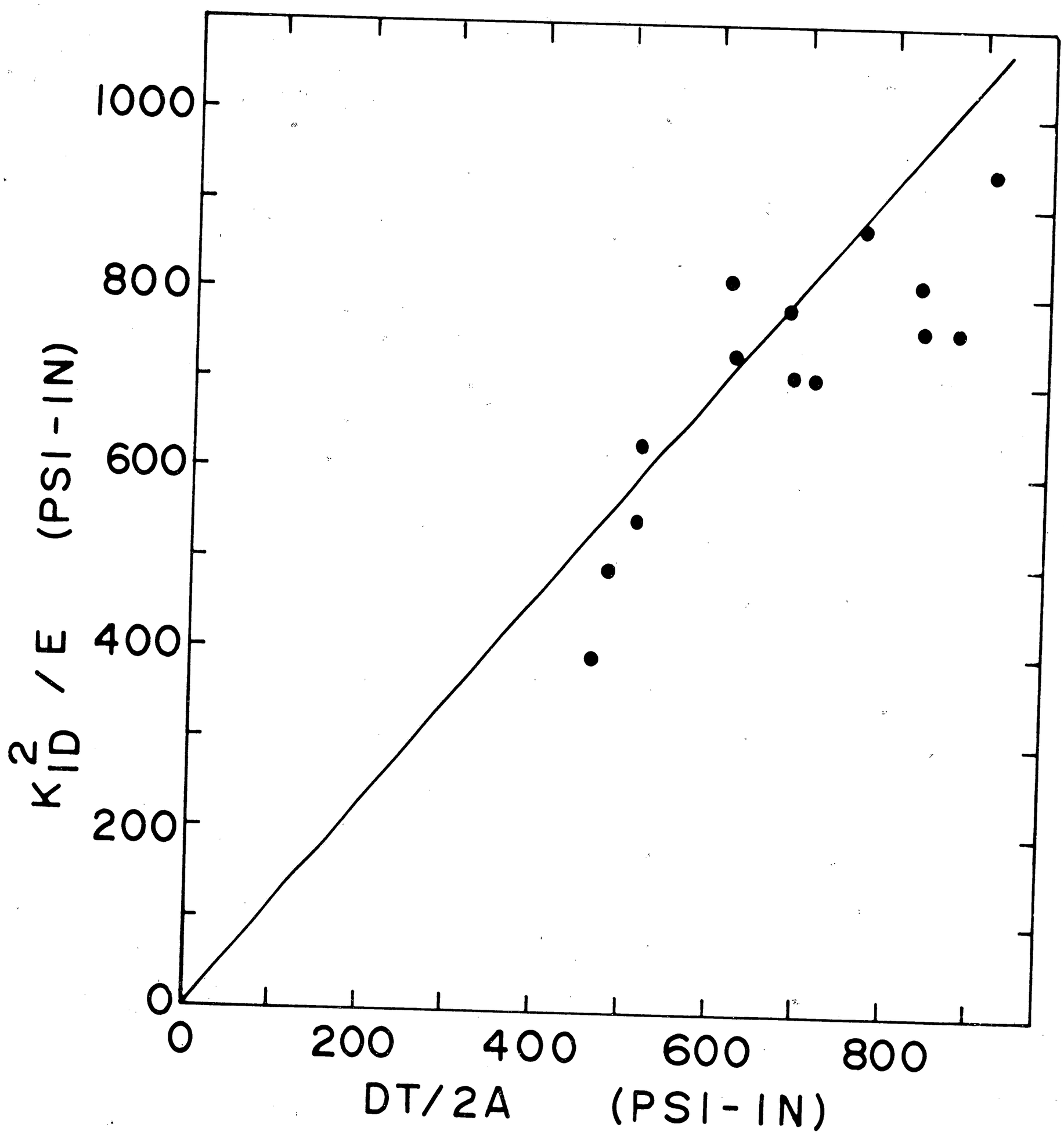

Figure 25 — Correlation of K_{ID} and DT on the Basis of Strain Energy Release Rate

For the computation of DT/2A, actual fracture areas were used, these ranging from 2.62 sq. in. to 3.05 sq. in.

The correlation is good despite what appears to be significant deviation towards higher values of DT/2A. This simply represents the fact that the dynamic K values were corrected for plasticity while the DT values were not. Or from another standpoint, it represents the condition discussed in the introduction in which for ductile materials the energy rate required for initiation of the fracture is less than that required for fracture to continue once initiation has occurred. The only deviation towards a higher value of K_{1D}^2/E was specimen number 3 which had an a/W value which probably exceeded the limits of the elastic analysis on which equations (5) and (6) were based.

The ultimate test of the correlation is the ability to use DT and tensile data to determine a K_{QD} value which when corrected for plasticity would yield an accurate value of K_{1D}. This procedure would be represented by the following series of equations:

$$K_{QD} = \left[\frac{E}{1-u^2} \cdot \frac{DT}{2A}\right]^{\frac{1}{2}} \tag{23}$$

$$\beta = \frac{1}{B}\left(\frac{K_{QD}}{YD}\right)^2 \tag{24}$$

$$K_{iD} = \left[\frac{K_{QD}^2}{1 + .5\beta}\right]^{\frac{1}{2}} \tag{25}$$

This procedure was carried out with the DT and tensile data of Tables VI and X using the average elastic modulus for each group, a value of u = 0.37 and the static yield strength corrected by equation (20). The results are shown in Table XI and Figure 26. The relative error shown in column 5 was computed using the equation:

$$r_e = \frac{K_t - K_c}{K_t} \times 100 \qquad (26)$$

where K_t is the true value of K_{1D} from Table IX and K_c is that calculated using equations (23) through (25). Eight of the calculated values had a relative error of 6.7% or less. Only two exceeded 10.6%, those being in Group I where as previously mentioned the input energies for the tests were quite high resulting in questionable DT values.

Group No.	Spec. No.	Calculated K_{1D}	True K_{1D}	Rel. Error %
I	1	112.6	114.6	1.7
	2	102.2	119.8	14.7
	3	97.5	115.6	15.6
II	5	119.9	119.9	0.0
	6	116.8	118.6	1.5
	7	115.6	123.9	6.7
III	9	112.3	125.0	10.1
	10	108.4	121.4	10.6
	11	109.3	116.2	5.9
	12	104.0	116.4	10.6
IV	13	91.9	100.5	8.4
	14	103.7	107.0	3.1
V	16	95.9	89.9	6.6
	17	100.9	109.9	8.0
	18	98.8	96.4	2.5

Table XI — Comparison of True Values of K_{1D} to those Predicted from DT Results

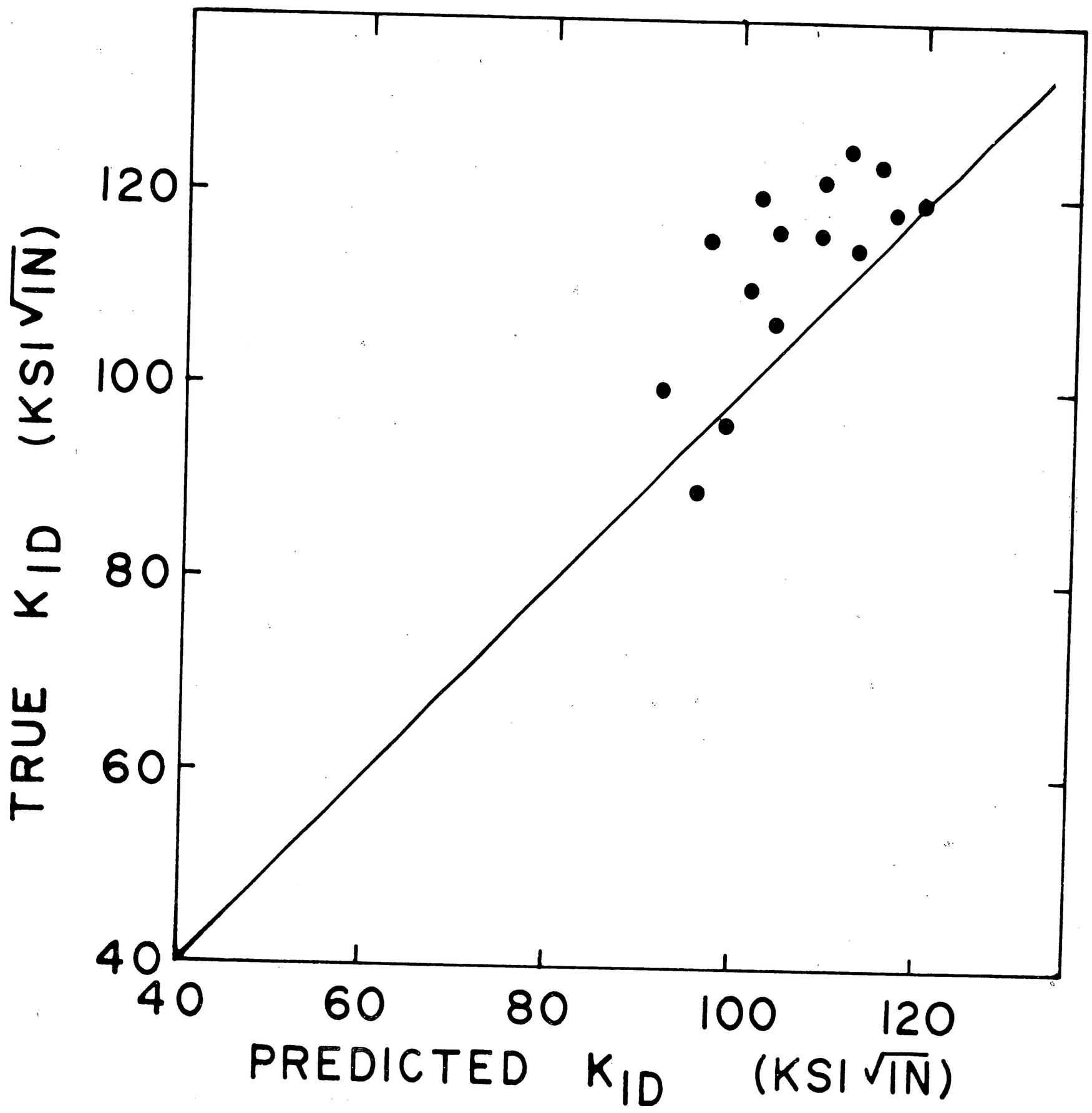

Figure 26 — Comparison of True K_{ID} with that Predicted from DT Energy

Note particularly that specimens 5 and 6 which had the greatest deviation towards higher values of DT/2A in Figure 25, in fact, were predicted with the greatest accuracy.

CONCLUSIONS

Based on the results of this investigation, the following conclusions may be drawn for the test material, Ti-6Al-4V:

1. The dynamic plane strain fracture toughness of the alloy exceeds its static fracture toughness by a factor of approximately two.

2. Dynamic plane strain fracture toughness can be analytically related to dynamic tear energy on the basis of strain energy release rate. Through this relationship, K_{1D} values can be predicted from DT energy with an accuracy of approximately 10% which is significantly better than the accuracy of graphical K_{1C} - DT correlations.

3. The effect of temperature and strain rate on the alloy's yield strength is subject to numerical description quite similar to that developed for plain carbon steels.

4. The alloy does not respond well to solution treatment in one inch thick section. However, within the same plate of the size tested, excellent reproducibility of mechanical test results is possible.

APPENDIX A

Sample Calculation of K_{1D}

The data for specimen number 10 will be used for the sample calculation of K_{1D}:

S	= 15.96 in.	P	= 48.12 kips
B	= 1.004 in.	σ_{YS}	= 158.6 ksi
a	= 1.69 in.	$\dot{e}$	= 75 sec^{-1}
W	= 4.712 in.	Y	= 1.950

First, using equation (5) to calculate K_{QD}:

$$K_{QD} = \frac{1.5\ PS(a)^{\frac{1}{2}}}{BW^2}\ Y$$

$$= \frac{1.5(48.12)(15.96)(1.69)^{\frac{1}{2}}}{(1.004)(4.712)^2} \cdot 1.950$$

$$= 131.00\ \text{ksi-in}^{\frac{1}{2}} \qquad \text{(A1)}$$

For determining r_p and beta, the dynamic yield strength is calculated using equation (20):

$$\sigma_{YD} = \sigma_{YS} + 4 + 8 \log \dot{e}$$

$$= 158.6 + 4 + 8 \log 75$$

$$= 177.6\ \text{ksi} \qquad \text{(A2)}$$

The plastic zone correction, from equation (7) is then:

$$r_p = \frac{1}{2\pi}\left(\frac{K_{QD}}{\sigma_{YD}}\right)^2$$

$$= \frac{1}{2\pi}\left(\frac{131.00}{177.6}\right)^2$$

$$= .086 \text{ in.} \qquad \text{(A3)}$$

The effective crack length using equation (8) is:

$$a_1 = a + r_p$$

$$= 1.69 + .086$$

$$= 1.776 \text{ in.} \qquad \text{(A4)}$$

Using a_1 and its associated value of $f(a/W)$ to calculate a corrected K_{QD} we have from equation (5):

$$K_{QD} = \frac{1.5(48.12)(15.96)(1.776)^{\frac{1}{2}}}{(1.004)(4.712)^2} \quad 2.000$$

$$= 137.74 \text{ ksi-in}^{\frac{1}{2}} \qquad \text{(A5)}$$

The plasticity correction β is determined using equation (10):

$$\beta = \frac{1}{B}\left(\frac{K_{QD}}{\sigma_{YD}}\right)^2$$

$$= \frac{1}{1.004}\left(\frac{137.74}{177.6}\right)^2$$

$$= .607 \qquad \text{(A6)}$$

The plasticity correction (β) is then used to obtain K_{1D} from the corrected K_{QD} value using equation (9):

$$K_{1D} = \frac{K_{QD}}{\sqrt{1 + .5\beta}}$$

$$= \frac{137.74}{\sqrt{1 + .5(.607)}}$$

$$= 121.44 \text{ ksi-in}^{\frac{1}{2}} \qquad \text{(A7)}$$

APPENDIX B

Development of the Relationship Between Dynamic Tear Energy and Impulse

The kinetic energy of the weight when it strikes the specimen is equal to the potential energy of the weight before being released:

$$\tfrac{1}{2}mv_o^2 = Wh \qquad (B1)$$

The kinetic energy remaining in the weight after fracture of the specimen is $\frac{1}{2}mv^2$. The energy required for fracture (DT energy) is then:

$$DT = \tfrac{1}{2}mv_o^2 - \tfrac{1}{2}mv^2 \qquad (B2)$$

$$= \tfrac{1}{2}m\,(v_o^2 - v^2) \qquad (B2a)$$

Factoring:

$$DT = \tfrac{1}{2}m\,(v_o - v)(v_o + v) \qquad (B3)$$

Letting $v_o - v = \Delta v$,

$$DT = \tfrac{1}{2}m\Delta v(v_o + v) \qquad (B4)$$

Adding and subtracting v_o to the right hand side:

$$DT = \tfrac{1}{2}m\,v(2v_o + v - v_o) \qquad (B5)$$

And since $v_0 - v = \Delta v$,

$$DT = \tfrac{1}{2}m\Delta v(2v_0 - \Delta v) \tag{B6}$$

Removing the parentheses we have:

$$DT = m\Delta v\, v_0 - \frac{m^2\Delta v^2}{2m} \tag{B7}$$

Impulse is defined as $I = \int_{t_1}^{t_2} F\, dt$ and for very short time intervals it may be approximated by $I = m\Delta v$. Substituting this into equation (B7) we have:

$$DT = Iv_0 - \frac{I^2}{2m} \tag{B8}$$

or

$$DT = I\left(v_0 - \frac{I}{2m}\right) \tag{B9}$$

REFERENCES

1. Minkler, Ward W., "Industrial Uses Hold Key to Titanium's Future," *Metals Progress*, Vol. 102, No. 3 (1972), pp. 88-89.

2. Litvin, David A., and Smith, David E., "Titanium for Marine Applications," *Naval Engineers Journal*, Vol. 83, No. 5 (1971), pp. 37-44.

3. *Metals Handbook*, 8th Ed., Vol. 1, pp. 1148-1150, American Society for Metals, Metals Park, Ohio (1961).

4. Wu, K. C., and Lewis, R. E., "A Study of Weld Heat-Affected Zones in Ti-6Al-6V-2Sn Alloy," *Welding Journal*, June 1963, p. 241-S.

5. Ogden, H. R., and Holden, F. C., *Metallography of Titanium Alloys*, TML Report No. 103, 29 May 1958, Battelle Memorial Institute, Columbus, Ohio, pp. 2-4.

6. Curtis, R. E., and Spurr, W. F., "Effect of Microstructure on the Fracture Properties of Titanium Alloys," *American Society for Metals Transactions*, Vol. 61 (1968), pp. 115-127.

7. Williams, J. C., and Blackburn, M. J., "A Comparison of Phase Transformation in Three Commercial Titanium Alloys," *American Society for Metals Transactions*, Vol. 60 (1967), pp. 373-383.

8. Goode, R. J., Judy, R. W., Jr., and Huber, R. W., *Procedures for Fracture Toughness Characterization and Interpretations to Failure-Safe Design of Structural Titanium Alloys*, NRL Report 6779, 5 December 1968, Naval Research Laboratory, Washington, D.C.

9. Lang, E. A., and Loss, F. J., "Dynamic Tear Energy — A Practical Performance Criterion for Fracture Resistance," *Impact Testing of Metals*, ASTM STP 466, American Society for Testing and Materials, 1970, pp. 241-258.

10. Paris, Paul C., and Sih, George C., "Stress Analysis of Cracks," *Fracture Toughness Testing and Its Applications*, ASTM STP 381, American Society for Testing and Materials, 1965, pp. 30-81.

11. Luft, David E., Madison, Ronald B., and Irvin, G. R., *Measurement of Dynamic K_C from the Drop Weight Tear Test*, Fritz Engineering Laboratory Report 335.1, 1968, Lehigh University, Bethlehem, Penna.

12. Judy, R. W., Freed, C. N., and Goode, R. J., *A Characterization of the Fracture Resistance of Thick Section Titanium Alloys*, NRL Report 7427, 5 July 1972, Naval Research Laboratory, Washington, D.C.

13. Irwin, G. R., and Krafft, J. M., *Basic Aspects of Crack Growth and Fracture*, NRL Report 6598, 21 November 1967, Naval Research Laboratory, Washington, D.C.

14. Freed, C. N., and Goode, R. J., *Correlation of Two Fracture Toughness Tests for Titanium and Ferrous Alloys*, NRL Report 6740, 16 January 1969, Naval Research Laboratory, Washington, D.C.

15. Judy, R. W., Jr., Goode, R. J., and Freed, C. N., *Fracture Toughness Characterization Procedures and Interpretations to Fracture-Safe Design of Structural Aluminum Alloys*, NRL Report 6871, 31 March 1969, Naval Research Laboratory, Washington, D.C.

16. Pellini, W. S., and Loss, F. L., *Integration of Metallurgical and Fracture Mechanics Concepts Relating to Fracture-Safe Design of Structural Steels*, NRL Report 6900, 22 April 1969, Naval Research Laboratory, Washington, D.C.

17. Krafft, J. M., and Irwin, G. R., "Crack Velocity Considerations," *Fracture Toughness Testing and Its Applications*, ASTM STP 381, American Society for Testing and Materials, 1965, pp. 114-129.

18. Hahn, G. T., Hoaglund, R. G., and Rosenfield, A. R., "The Variation of K_{1C} with Temperature and Loading Rate," *Metallurgical Transactions*, Vol. 2, 1971, p. 537.

19. Ronald, T. M. F., Hall, J. A., and Pierce, C. M., "Usefulness of Precracked Charpy Specimens for Fracture Toughness Screen Test for Titanium Alloys," *Metallurgical Transactions*, Vol. 3, 1972, p. 813.

20. "Tentative Method of Test for Plane Strain Fracture Toughness of Metallic Materials," *Review of Developments in Plane Strain Fracture Toughness Testing*, ASTM STP 463, American Society for Testing and Materials, 1970, pp. 249-269.

21. Gerberich, W. W., and Baker, G. S., "Toughness of Two-Phase 6Al-4V Titanium Microstructures," *Related Phenomena in Titanium Alloys*, ASTM STP 432, American Society for Testing and Materials, 1968, pp. 80-99.

22. *Metals Handbook*, 8th Ed., Vol. 7, p. 329, American Society for Metals, Metals Park, Ohio, 1972.

23. Freed, C. N., "A Comparison of Fracture Toughness Parameters for Titanium Alloys," *Engineering Fracture Mechanics*, Vol. 1, pp. 125-189, 1968.

24. Wood, R. A., *DMIC Review of Recent Developments: Titanium and Titanium Alloys*, Defense Metals Information Center, Battelle Memorial Institute, Columbus, Ohio, 29 August, 1971.

25. Harrigan, M. J., Sommer, A. W., and Alers, G. A., *The Effect of Texture on the Mechanical Properties of Titanium Alloys*, Report NA-69-909, North American Rockwell Corp., Los Angeles, Calif., December 1969.

26. Vishnevsky, C., and Steigerwald, E. A., "Plane Strain Fracture Toughness of Some Cyrogenic Materials at Room and Subzero Temperatures," *Fracture Toughness Testing at Cyrogenic Temperatures*, STP 496, American Society for Testing and Materials, 1971, pp. 3-26.

27. Shamblen, C. E., "Embrittlement of Titanium Alloys by Long Time High Temperature Exposure," *Metallurgical Transactions*, Vol. 2, p. 277, 1971.

28. Greist, A. J., Doig, J. R., and Frost, P. D., "Correlation of Transformation Behavior with Mechanical Properties of Several Titanium Alloys," *Transactions of the Metallurgical Society of the AIME*, Vol. 215, pp. 627-632, 1959.

29. Dupouy, J. M., Bever, M. B., and Averbach, B. L., "On the Ageing Behavior of the Alloy Ti-6Al-4V," *American Society for Metals Transactions*, Vol. 52, pp. 221-233, 1960.

30. Sherman, R. G., and Kessler, H. D., "Investigation of the Heat Treatability of Ti-6Al-4V," *American Society for Metals Transactions*, Vol. 48, pp. 657-676, 1956.

31. Puzak, P. P., and Lange, E. A., *Standard Method for the 1-Inch Dynamic Tear Test*, NRL Report 6851, Naval Research Laboratory, Washington, D.C., 13 February 1969.

32. Pellini, W. S., *Evolution of Engineering Principles for Fracture-Safe Design of Steel Structures*, NRL Report 6957, Naval Research Laboratory, Washington, D.C., 23 September 1969.

33. Rosenfield, A. R., and Hahn, G. T., "Numerical Descriptions of the Ambient Low Temperature and High Strain Rate Flow and Fracture Behavior of Plain Carbon Steel," *American Society for Metals Transactions*, Vol. 59, pp. 962-980, 1966.

34. Steidel, R. F., and Makerov, C. E., "Tensile Properties of Some Engineering Materials at Moderate Strain Rates," *American Society for Testing and Materials Bulletin*, Vol. 247, p. 57, 1960.

35. Mardirosian, M. M., and Riffin, P. V., *Strain Rate Effects in Brittle Materials*, ASM Technical Report C70-16.3, American Society for Metals, 1970.

36. Maykuth, D. J., Monroe, R. E., Favor, R. J., and Moon, D. P., *Ti-6Al-4V Handbook*, Defense Metals Information Center, Battelle Memorial Institute, Columbus, Ohio, 1971.

VITA

George F. Mitchell was born in New Bern, North Carolina on 22 January 1941. He attended public school in Baltimore, Maryland, graduating from Baltimore Polytechnic Institute in 1959. In 1964 he received a Bachelor of Science Degree from the U. S. Naval Academy and was commissioned into the Naval Service. Lieutenant Commander Mitchell attended Lehigh University under the Advanced Science Program sponsored by the United States Navy.